Excitation Energy Calculations with TD-DFT

Dissertation

zur

Erlangung der wissenschaftlichen Doktorwürde
(Dr. Sc. Nat)

vorgelegt der

Mathematisch-naturwissenschaftlichen Fakultät

der

Universität Zürich

von

Thomas Chassaing

von

Masein GR

Promotionskomitee

Prof. Dr. Jürg Hutter (Vorsitz)

Prof. Dr. Michiel Sprik

Zürich, 2005

Contents

Abstract

Quantitative calculations of the electronic structure of matter are being done ever since the inception of quantum mechanics. But the high number of degrees of freedom involved puts strict limits on the number of electrons, that can be treated with present day computers. Even using strong approximations, the so-called quantum chemical methods, which basically solve the Schrödinger equation, are barely able to handle systems consisting of about 100 atoms. Density functional theory (DFT), with roots dating back the 1930's but firmly established in 1964 by the Hohenberg-Kohn theorem, uses the electronic density, rather than the electronic wavefunction, as the basic variable. This reduces the number of degrees of freedom to three and thus allows for the calculation of large systems of up to thousands of atoms. In the Kohn-Sham formalism, the most widely used version of DFT, the system of interacting electrons is replaced by a system of non-interacting electrons in an effective potential. This allows to easily compute the kinetic energy of the non-interacting system, which closely approximates kinetic energy of the interacting system. The kinetic energy, of the non-interacting system, plus the averaged Coulomb energy and the interaction energy with the external potential (the electron-nucleus attraction for example) make up the largest part of the energy of the system. The remaining part defines the exchange-correlation energy. This functional is not explicitly known however and has to be approximated. With approximate exchange-correlation functionals depending on the gradient of the electronic density, the accuracy of DFT has become good enough for chemical applications. DFT is now a well established theory, widely used in a variety of scientific fields, such as chemistry, molecular biology, the investigation of superconductivity, semiconducter physics, and many others.

In its original form, DFT is applicable only to ground-states. The Runge-Gross theorem extends the theory into the time-domain, called time-dependent DFT (TD-DFT), and thus allows the

treatment of electronically excited states. In combination with linear response theory, recently complete formulations of excited state calculations in molecular and extended systems were given.

Implementations can be roughly classified into molecular codes and condensed matter codes. The former use localization techniques to model the restricted spatial extend of the systems treated. The latter use delocalized expansion functions that are adapted to the infinitely extended systems under investigation. Some systems of interest, though, have both molecular and condensed phase characteristics, think, for example, of diluted solutions. In fact, it is possible to calculate molecules with condensed matter codes and vice versa, but typically the accuracy in such situations is very limited due to the inefficient use of computer resources in these cases. Codes that use both, localized and delocalized expansion functions can handle molecules and condensed matter equally well and are suited for liquid systems as well.

In this thesis the following contributions, regarding electronic excitation energy calculations using TD-DFT, are made:

Chapter 3 presents the implementation of the excitation energy linear response equations in the framework of the Gaussians and plane waves (GPW) method. This method uses Gaussian functions to expand the electronic orbitals and plane waves to expand the electronic density. The result is a code, that can handle all types of systems efficiently. The accuracy of the TD-DFT implementation in the GPW framework is accessed by comparison with an established molecular code. A good agreement is found for the tested set of small molecules.

In the next chapter 4, the implementation of the TD-DFT equations is extended to the Gaussian and augmented plane waves (GAPW) method. This method addresses the issue, that the delocalized plane waves are not the ideal choice for the expansion core or semi-core electrons. The GAPW method therefore uses both localized and delocalized functions for the expansion of the electronic density. A compensation density and compensating multipole terms facilitate the numerical handling of the method. Test calculations show that the TD-DFT GAPW implementation gives the same values as the GPW method.

It was mentioned, that ground-state properties are predicted to a high accuracy in DFT when using gradient corrected exchange-correlation functionals. This is, however, not true for all excitation energies. The class of, so-called, Rydberg excitations are severely underestimated if

these standard functionals are employed. It has been found, that the problem lies with incorrect shape of the exchange-correlation potential, which results from the exchange-correlation functional. Several proposals have been made to improve these Rydberg values by improving the representation of the exchange-correlation potential in the region of the involved Kohn-Sham orbitals. These potentials do not have a corresponding functional however and thus the total energy of the ground- and excited states is not available. Furthermore, these potentials are computationally very expensive and break the linear scaling behavior of the GPW or GAPW method. In chapter 5 the two-step procedure, which applies the corrected potential in an approximate way is proposed. Thereby we achieve a much smaller computational cost than would be possible if the corrected potential would be fully applied. The two-step procedure works in the following way: first a standard DFT calculation is done, to obtain the ground-state density, which is used in the TD-DFT calculation. In the second step, the corrected potential is evaluated using the density from the first step and the TD-DFT calculation is performed. The difference to the full application of the corrected potential is, that the ground-state density is not allowed to relax under the influence of the corrected potential, which would require many successive applications of the corrected potential. Since the corrected potential is applied only once in the two-step procedure, the computational cost is much lower. Because a standard exchange-correlation functional is used in the ground-state calculation, the total energy is still defined when using the two-step procedure. We find that the two-step procedure is indeed capable of giving improved excitation energies for the Rydberg excitations, but it also gives slightly worse results for other types of excitations. However, the excitation energies are not as good as the ones obtained by applying the corrected potential self-consistently.

The methods presented in this work can serve as a starting point for further implementations of response properties, for example the calculation of X-ray absorption spectra or of NMR chemical shifts.

Zusammenfassung

Quantitative Berechnungen der Elektronenstruktur der Materie werden schon seit den Anfängen der Quantenmechanik gemacht. Jedoch beschränkt die dabei auftretende hohe Zahl an Freiheitsgraden die Zahl der Elektronen, die mit heutigen Computern behandelt werden können. Die sogenannten quantenchemischen Methoden, die im Wesentlichen die Schrödingergleichung lösen, können, selbst bei groben Näherungen, liegen Systeme von 100 Atomen an der Obergrenze der Berechenbarkeit. Die Dichtefunktionaltheorie (DFT), deren Wurzeln bis in die 1930er Jahre zurückgehen und die 1964 mit dem Hohenberg-Kohn Theorem fest etabliert wurde, benutzt als grundlegende Variable die Elektronendichte, statt der elektronischen Wellenfunktion. Dies reduziert die Anzahl der vorkommenden Freiheitsgrade auf drei und erlaubt somit die Berechnung von Systemen mit mehr als Tausend Atomen. In der am häufigsten benutzten Version der DFT, dem Kohn-Sham Formalismus, wird das System von wechselwirkenden Elektronen auf ein System nicht wechselwirkender Elektronen, die sich in einem effektiven Potential bewegen, abgebildet. Dies macht es einfach, den Beitrag der kinetischen Energie des nicht wechselwirkenden Systems, der eine gute Näherung für die kinetische Energie des wechselwirkenden Systems darstellt, näherungsweise zu berechnen. Die kinetische Energie des nicht wechselwirkenden Systems plus die gemittelte Coulomb-Wechselwirkung und die Wechselwirkung mit dem externen Potential (zum Beispiel die Elektron-Kern Anziehung) haben den grössten Anteil an der totalen Energie des Systems. Der Rest definiert die sogenannte Austausch-Korrelations Energie. Das Funktional der Austausch-Korrelations Energie ist nicht bekannt und muss angenähert werden. Mit Näherungen, die vom Gradienten der Dichte abhängen, hat die DFT eine Genaugkeit erreicht, die sie für chemische Anwendungen nutzbar macht. Mittlerweile ist die DFT eine gut eingeführte Theorie, die in einer grossen Anzahl von wissenschaftlichen Gebieten Anwendung findet, so zum Beispiel in der Molekularbiologie, der Untersuchung von Supraleitern, in der

Halbleiterphysik und in anderen Bereichen.

In ihrer Ursprünglichen Form ist die DFT nur für Grundzustandsrechnungen geeignet. Das Runge-Gross Theorem erweitert die Theorie jedoch für Zeitabhängige Phänomene, zeitabhängige DFT (TD-DFT vom englischen time-dependent DFT) genannt, und erlaubt somit die Behandlung von angeregten Zuständen. Kürzlich wurden Formeln für die Berechnung von elektronisch angeregten Zuständen von Molekülen und von ausgedehnten Systemen vorgestellt, die TD-DFT zusammen mit der linear response Theorie benutzen.

Computerausführungen der DFT können grob in Programme für die Berechnung von Molekülen und solche für die Berechnung von kondensierter Materie aufgeteilt werden. Die Ersteren benutzen Lokalisierungstechniken um der begrenzten Ausdehnung der Systeme Rechnung zu tragen. Die Programme für kondensierte Materie tragen der grossen, möglicherweise unendlichen Ausdehung dieser Systeme Rechnung indem sie delokalisierte Entwicklungsfunktionen verwenden. Einige interessante Systeme haben jedoch sowohl molekularen als auch kondensierten Charakter, man denke zum Beispiel an verdünnte Lösungen. Zwar ist es möglich, Moleküle mit Programmen für kondensierte Materie zu berechnen und umgekehrt, doch ist die Genauigkeit eines solchen Vorgehens typischerweise eher schlecht, aufgrund der ineffizienten Nutzung der Computerressourcen. Programme die beides, lokalisierte und delokalisierte Entwicklungsfunktionen, einsetzen, können Moleküle und kondensierte Materie gleichermassen gut behandeln und eignen sich somit auch für flüssige Systeme.

In dieser Dissertation werden nachfolgende Beiträge zur Berechnung der elektronischen Anregungsenergien mit TD-DFT gemacht:

Kapitel 3 beschreibt die Ausführung der linear response Gleichungen zur Berechnung der elektronischen Anregungsenergien im Rahmen der Gauss- und ebene Wellen Funktionen (GPW vom englischen Gaussian and plane waves) Methode. Diese Methode entwickelt die elektronischen Orbitale mit Hilfe von Gauss-Funktionen und die Elektronendichte mit Hilfe von ebenen Wellen. Daraus resultiert ein Programm, das alle Arten von Systemen effizient berechnen kann. Die Exaktheit der TD-DFT Implementierung mittels der GPW Methode wird im Vergleich mit einem bewährten molekularen Programm getestet. Die Berechnungen an einem Satz von kleinen Molekülen zeigen eine gute Übereinstimmung.

Das darauffolgende Kapitel 4 zeigt die Ausführung der TD-DFT Gleichungen im Rahmen der

“Gaussian and augmented plane waves” (GAPW) Methode, was soviel wie Gauss- und erweiterte ebene Wellen Funktionen heisst. Die ebenen Wellen sind nicht die am besten geeigneten Funktionen, um die kernnahen Zustände zu entwickeln. Deshalb verwendet die GAPW Methode sowohl lokalisierte, als auch delokalisierte Funktionen, um die Elektronendichte zu entwickeln. Die numerische Handhabung der Methode wird durch Kompensationsdichten und -multipole vereinfacht. Testrechnungen belegen, dass die GAPW Methode dieselben Resultate liefert wie die GPW Methode.

Es wurde erwähnt, dass die DFT zusammen mit Gradienten korrigierten Austausch-Korrelations Funktionalen Eigenschaften im Grundzustand mit hoher Präzision berechnen kann. Dies gilt jedoch nicht für alle elektronisch angeregten Zustände. Für die Klasse der sogenannten Rydberg Anregungen, werden viel zu tiefe Anregungsenergien vorhergesagt, wenn man Standard Austausch-Korrelations Funktionale einsetzt. Es wurde entdeckt, dass dies an der inkorrekten Form des Austausch-Korrelations Potentials, welches sich aus dem Austausch-Korrelations Funktional ergibt, liegt. Es wurden verschiedene Vorschläge gemacht, die die Genauigkeit des Austausch-Korrelations Potentials in den relevanten Bereichen verbesseren. Diese korrigierten Potentiale haben jedoch kein korrespondierendes Austausch-Korrelations Funktional und deshalb können bei Verwendung dieser Potentiale die Energien des Grundzustandes und der angeregten Zustände nicht bestimmt werden. Ausserdem ist die Anwendung dieser Potentiale sehr rechenzeitintensiv und sie verschlechtern somit das sonst lineare Skalierungverhalten der GPW und GAPW Methoden. In Kapitel 5 wird die Zwei-Schritt Prozedur, welche ein korrigiertes Potential approximativ anwendet, vorgestellt. Somit wird ein geringerer Rechenaufwand erreicht, als wenn dass korrigierte Potential vollständig angewendet würde. Die Zwei-Schritt Prozedur funktioniert wie folgt: Zuerst wird eine DFT Rechnung mit einem Standard Funktional gemacht, um die Grundzustandsdichte zu bestimmen, die dann in der TD-DFT Rechnung benötigt wird. In einem zweiten Schritt wird das korrigierte Potential bestimmt und die TD-DFT Rechnung durchgeführt. Im Unterschied zur vollständigen Anwendung eines korrigierten Potentials kann sich die Grundzustandsdichte nicht an das korrigierte Potential anpassen. Dies würde nämlich die wiederholte Berechnung des korrigierten Potentials erfordern und somit einen viel höheren Rechenaufwand bedeuten. Weil die Zwei-Schritt Prozedur ein Standard Austausch-Korrelations Potential für die Grundzustandsberechnung benutzt, können die Energien des Grundzustands und der angeregten Zustände weiterhin berechnet werden.

Testrechnungen ergeben, dass die Zwei-Schritt Prozedur die berechneten Anregungsenergien der Rydbergzustände tatsächlich verbessert. Jedoch verschlechtern sich die Anregungenergien von anderen Zuständen etwas und die Resultate fallen schlechter aus, als wenn man die korrigierten Potentiale vollständig anwendet.

Die hier vorgestellten Methoden können als Ausgangspunkt für Programme zur Berechnung weiterer response Eigenschaften, zum Beispiel die Berechnung von Röntgen-Absorptionsspektren, oder von NMR chemical shifts, verwendet werden.

Chapter 1

Introduction

In his paper of 1900, Max Planck postulated that, at a microscopic level, matter can only take on specific states that have an energy which is a multiple of a fundamental energy content, the so-called "Plancksche Wirkungsquantum". This realization, which triggered the development of quantum theory, was motivated by the need to have a theory which is consistent with the experimental data provided by the, at that time, relatively new methodology of spectroscopy. Spectroscopy is concerned with the study of the absorption and emission of light by matter. As Planck found out correctly, this emission and absorption processes are nothing but the transitions between different states of a quantum system. We call the state of the lowest possible energy the ground-state and all higher states excited states. If the transition is from a lower to a higher state, then this is called an excitation. If, on the other hand, the transition is from a higher state to a lower one, this is called a deexciation. Any system not in the ground-state is called to be in an excited state, or simply excited. Since the observation of spectra of molecules is a very important method to measure the properties of a quantum system, spectroscopy was of exceeding importance in the development of quantum theory and with it, of the whole of science. But the usefulness of spectroscopy lies not only in the power to verify quantum theory. Once the spectra of the molecules of interest are known, it also allows to identify the composition of a substance, an ability which is of importance in almost all the natural sciences. Chief among them is astronomy, which completely lacks the possibility of experiments and has to rely, for a large part, on spectroscopy to verify its theories. It is no wonder that many scientific field

evolved together with the understanding of spectroscopy.

There are several types of excitations possible in a system of atoms surrounded by electrons. Important are the vibrational and the electronic excitations. The first describe the energy increase due to the oscillating movement of the nuclei in the field of the electrons. Their energy usually ranges in the infrared band. The electronic excitations are due a change of state of the electrons in the potential of the nuclei and usually have higher corresponding energies in the visible to ultra-violet (UV) spectrum of light.

The usefulness of electronic excitations is not restricted to spectroscopy. The laser (light amplification through simultaneous emission of radiation) is a now indispensable invention that directly uses the theory of emission of light. The applications of laser technology are truly ubiquitous. Examples are, the entertainment industry with CD and DVD media and laser shows, the cosmetic industry with laser epilation, medical applications, where the laser is used as a very precise cutting tool, protection systems that use lasers for detection, the list could fill pages. With the ongoing miniaturization, nanotechnology is the word in everyone's mouth, production processes begin to protrude into the quantum realm. These production processes and products already have to take into account the interaction of radiation with matter and such nano-processes are going to become more and more important. On another track we have the life sciences, that have seen an incredible rise in popularity over the past decade (the 1990's). Today they are the most important scientific field, fundings-wise, and lots of effort is being poured into the quantum theoretical investigation of the live sustaining processes, mainly the functioning to the proteins. Arguably the most important processes in the circle of life on our planet, photosynthesis, involves the interaction of electromagnetic radiation of the sun, UV light, with a molecule called chlorophyll, a process which is believed to proceed via electronic excitations (charge-transfer excitation actually).

This thesis is about the calculation of electronic excitation spectra of matter. The interacting electric field is hereby modeled classically. This can be done, because the wavelength of the involved (optical) light is so large, that the corresponding electric field can be considered constant over the length of the molecule (or region of interest in a condensed system) [1]. This is somewhat

[1] At higher energies the quantum nature of the photon becomes important and a theory that can cope with the full range of relativistic effects (for example spontaneous emission of virtual electron-positron pairs), like quantum

analogous to the Born-Oppenheimer approximation, where the electrons and nuclei are treated at different levels of theory because of the large difference in mass of the two.

Unfortunately the Schrödinger equation, that describes the quantum world, can be solved analytically only for the most simple systems (H_2^+ being the most complicated and this only if the two hydrogen nuclei are considered attached to their positions). Still, attempts to calculate numerical solutions are as old as the theory itself. But the formidable complexity of the quantum equations forced people to find approximations that indeed were still impossible to solve analytically but could be tackled more easily. Early on there was the Hartree-Fock approximation which maps the full quantum problem onto a conceptually simpler one of independent electrons moving in the effective field of the other electrons. With the advent of the sheer calculating power of electronic computers the approximations could be more and more refined allowing to bring neglected interactions back into the calculation. Several methods to do this were developed, for example configuration interaction (CI), coupled cluster (CC), Møller-Plesseth (MP) perturbation theory, to only name the most prominent ones. These methods can now reach very high accuracy and provide a path to systematically improve the accuracy of the calculation by inclusion of ever more neglected interactions. Yet, they still have a tremendous computational cost, nominally scaling to the 4th and even larger power of the system size. Therefore only systems consisting of a few tens of atoms can be treated using these methods. For more information on these, so-called quantum chemical, methods, the reader is pointed to standard quantum chemistry textbooks such as [1] or [2].

A different method was proposed in the 1920's by Thomas [3] and Fermi [4] and in 1930 supplemented by Dirac [5]. The so-called Thomas-Fermi method uses the electronic density of the system as the fundamental variable and defines an energy functional of the density. In 1964 Hohenberg and Kohn [6] took up this idea and proved that all properties of a quantum system in the ground-state are a functional of the density of this same system, giving a formal justification of the Thomas-Fermi method. The use of the density, instead of the multi-particle wavefunction, reduces the number of degrees of freedom from $3 \times N$ to just 3, thus greatly reducing the complexity of the problem. One year later, Kohn and Sham [7] further proposed a mapping of the system of interacting electrons onto a set of non-interacting electrons moving in an effective field. This trick allows to find good approximations for the unknown energy functional. The theory

field theory, has to be used.

of density functionals became known as density functional theory (DFT) and the mapping onto independent electrons as the Kohn-Sham (KS) formalism. Because of it's computational ease, DFT, and especially KS-DFT, has become exceedingly popular, culminating in the Nobel prize for W. Kohn in 1998 (together with J. A. Pople, who was honored for his contributions to quantum chemistry) and papers on DFT are now among the most cited in science. The drawback of DFT is, that the functional of the density is not explicitly known, and there is no way to systematically improve the approximations currently used.

Standard DFT is not suitable for excited state calculations though, because the Hohenberg-Kohn theorem is only valid for ground-states. Nevertheless, one can try to find properties of excited states, in the KS formalism, by specifying occupation levels of the independent electron system and doing so-called ΔSCF calculations, where the difference between the calculation with the specified occupancy and the ground-state system is taken. Another possibility are the finite difference methods, where the response to a perturbation (an electromagnetic field, for example) in question is found by calculating the energy of the system for different finite values of the perturbation and then taking the numerical derivative. These methods are straightforward in the sense, that standard ground-state DFT can be applied. They merely require the calculation of several ground-state energies and then taking the difference of them by the user. But they are also only crude workarounds for a theory that would allow for multiple states and a time-evolution of the system. This theory is now known as time-dependent DFT (TD-DFT). The first applications of TD-DFT actually preceeded its rigorous formal foundation. Zangwill and Soven [8] calculated photo-absorption cross sections and static polarizabilities of rare gases using a self-consistent KS-type method in 1980. Further steps towards a rigorous formulation of TD-DFT were taken by Deb and Ghosh [9] and Bartolotti [10, 11, 12, 13] but these derivations were limited to special time-dependent potentials. In 1984 Runge and Gross provided the extension of the Hohenberg-Kohn theorem to the time-dependent domain [14]. Almost ten years later, in 1995, Casida published a molecular algorithm for TD-DFT using response theory (TD-DFRT) [15]. This spurred a whole list of TD-DFRT codes, and with them calculations of different response properties of fairly large systems, up to hundreds of atoms, have become routine.

But all is not well. The problems of DFT, the self-interaction error (SIE) for example, also affect TD-DFRT. And TD-DFRT has it's own shortcomings: The occurrence of a further functional requires more approximations, the SIE affects certain TD-DFRT calculations severely (more on

this in chapter 5), current TD-DFRT calculations fail for so-called charge-transfer excitations, and there is more.

The structure of this document is as follows. In chapter 2 the theory of TD-DFRT is presented and the approximations to the involved density functionals are briefly discussed. Chapter 3 presents the Gaussian and plane wave implementation of TD-DFRT, a code capable of doing linear scaling calculations and thus allowing for TD-DFRT calculations in systems with thousands of atoms. Chapter 4 presents the implementation of TD-DFRT within the Gaussian and augmented plane waves framework. This novel method allows linear scaling calculations in an all-electron system, using the tried and true techniques of the GPW and localized functions methods. The next chapter, 5, describes a new method to improve the calculated excitation energies in a efficient way. Chapter 6 draws the conclusions of this work and gives an outlook of possible future developments related to this work. The thesis is completed with an appendix, giving details of the calculations involving functional derivatives and some definition of terms.

Chapter 2

Time-dependent density functional response theory

In this chapter the basic time-dependent density functional response theory is laid out. Knowledge of ground-state DFT in the Kohn-Sham formulation (see, for example, [16, 17]) is assumed. Reviews of TD-DFT can be found in [15] or [18] for example.

2.1 Time-dependent density functional theory

Consider a system of atoms or molecules with fixed nuclei and a time-dependent external potential. The time-dependent electronic wavefunction is described by the time-dependent Schrödinger equation. The Runge-Gross [14] theorem is then the analogue of the Hohenberg-Kohn theorem for the time-dependent system. It states that, under certain conditions and for a given initial state, a one to one mapping between the time-dependent charge density and the external potential exists. Based on this, a functional of the density can be constructed, which has a stationary point at the true time-dependent density. As in the ground-state case, the system can be mapped onto a set of non-interacting electrons, moving in an effective potential. In this section the development of the arguments largely follow the Runge-Gross [14] paper.

2.1.1 The Runge-Gross theorem

The time-dependent Schrödinger equation for a system of N electrons is (atomic units used throughout this work)

$$\hat{H}(t)\Psi(t) = i\frac{\partial}{\partial t}\Psi(t) \tag{2.1}$$

with the Hamiltonian

$$\hat{H}(t) = \hat{T} + V(t) + W. \tag{2.2}$$

$\Psi(t)$ is the many particle wavefunction (spatial coordinates are omitted for brevity whenever possible), $\hat{T}$ is the kinetic energy operator

$$\hat{T} = \sum_{i=1}^{N} -\frac{1}{2}\nabla_i^2, \tag{2.3}$$

$V(t)$ is the time-dependent external potential usually containing the potential of the nuclei

$$V(t) = \sum_{i=1}^{N} v(r_i, t), \tag{2.4}$$

and W is the electron-electron repulsion

$$W = \sum_{i<j} \frac{1}{|r_i - r_j|}. \tag{2.5}$$

By solving the Schrödinger equation for different external potentials $V(t)$ and a *fixed* initial state Ψ^0, a mapping $G : v(r,t) \rightarrow n(t)$ from the external potential to the charge density

$$n(r,t) = \int dr_2 \dots dr_N \; \bar{\Psi}(r, r_2, \dots, r_N, t)\Psi(r, r_2, \dots, r_N, t) \tag{2.6}$$

is generated[1].

The Runge-Gross theorem states, that this map G is invertible $G^{-1} : n(r,t) \rightarrow v(r,t) + C(t)$ up to a purely time-dependent function $C(t)$, if the single-particle potential $v(r,t)$ is expandable into a Taylor series around $t = t_0$ with respect to the time coordinate. The time-dependent

[1] In this document, whenever there is an integral over space coordinates for which there are no limits, the integral runs over all space.

function $C(t)$ will change the electronic wavefunction only by a time-dependent phase factor $\tilde{\Psi}(t) = e^{-i\alpha(t)}\Psi(t)$ with $\dot{\alpha}(t) = C(t)$. But the phase factor does not contribute to the expectation values of operators which do not contain derivatives with respect to time $\langle\tilde{\Psi}(t)|\hat{O}|\tilde{\Psi}(t)\rangle = \langle\Psi(t)|\hat{O}|\Psi(t)\rangle$. In other words, the density of a time-dependent system determines the time-dependent potential, which in turn determines the time-dependent wavefunction and thus every, physically meaningful, expectation value can be regarded as a functional of the density, provided the aforementioned conditions are respected.

In analogy to the time-independent case, where an energy functional $E[n]$ is defined, an action functional $A[n]$ is defined

$$A[n] = \int_{t_0}^{t_1} dt\langle\Psi[n](t)|i\frac{\partial}{\partial t} - \hat{H}(t)|\Psi[n](t)\rangle = B[n] - \int_{t_0}^{t_1} dt \int d^3r\, n(r,t)v(r,t). \tag{2.7}$$

The action functional $A[n]$ of equation (2.7) is split into a universal part $B[n]$, characterized by an analytic expression which is independent of the system, and and a part depending on the external potential. $B[n]$ is defined as

$$B[n] = \int_{t_0}^{t_1} dt\langle\Psi[n](t)|i\frac{\partial}{\partial t} - \hat{T} - W|\Psi[n](t)\rangle \tag{2.8}$$

In the Runge-Gross paper it is stated that, in general, the action integral $A[n]$ doesn't have a minimum but has a stationary point at the solution of the Schrödinger equation (2.1). This is in contrast to the the time-independent case, where the exact solution corresponds to an absolute minimum of the energy functional $E[n]$. Therefore, the exact time-dependent density can be obtained by applying the variational principle

$$\frac{\delta A}{\delta n(t)} = 0. \tag{2.9}$$

Let's define a new functional $S_W[n]$

$$S_W[n] = \int_{t_0}^{t_1} dt\langle\Psi[n](t)|i\frac{\partial}{\partial t} - \hat{T}|\Psi[n](t)\rangle \tag{2.10}$$

that depends parametrically on the electron-electron interaction W through the dependence of $\Psi(t)$ on W. $S_0[n]$ then corresponds to the special case of non-interacting particles.

Using $S_W[n]$, the action integral is rewritten as

$$A[n] = S_0[n] - \frac{1}{2}\int_{t_0}^{t_1} dt \int d^3r \int d^3r' \frac{n(r,t)n(r',t)}{|r-r'|} - \int_{t_0}^{t_1} dt \int d^3r\, n(r,t)v(r,t) - \underbrace{\left\{(S_0[n] - S_W[n]) - \frac{1}{2}\int_{t_0}^{t_1} dt \int d^3r \int d^3r' \frac{n(r,t)n(r',t)}{|r-r'|} + \int_{t_0}^{t_1} dt \langle \Psi[n](t)|W|\Psi[n](t)\rangle\right\}}_{A^{\mathrm{xc}}[n]} \tag{2.11}$$

from which we extract the definition of the exchange-correlation action functional $A^{\mathrm{xc}}[n]$.

2.1.2 Time-dependent Kohn-Sham equations

To derive the time-dependent Kohn-Sham equations a set of non-interacting electrons, described by single-particle wavefunctions $\{\phi_i(t)\}$, also called orbitals, is postulated. The total electronic wavefunction is taken to be a Slater-determinant of these single-particle orbitals

$$\Psi(t) = \frac{1}{\sqrt{N!}} \begin{vmatrix} \phi_1(r_1,t) & \phi_2(r_1,t) & \cdots & \phi_N(r_1,t) \\ \phi_1(r_2,t) & \phi_2(r_2,t) & \cdots & \phi_N(r_2,t) \\ \vdots & \vdots & \ddots & \vdots \\ \phi_1(r_N,t) & \phi_2(r_N,t) & \cdots & \phi_N(r_N,t) \end{vmatrix}. \tag{2.12}$$

The time-dependent density (2.6) then becomes

$$n(r,t) = \sum_{i=1}^{N} \overline{\phi_i}(r,t)\phi_i(r,t). \tag{2.13}$$

Taking the functional derivative of $A[n]$ to find the stationary point yields

$$\frac{\delta A[n]}{\delta n} = 0 = \frac{\delta S_0[n]}{\delta n} - \int d^3r' \frac{n(r',t)}{|r-r'|} - v(r,t) - \frac{\delta A_{xc}[n]}{\delta n}. \tag{2.14}$$

Carrying out the derivative of $S_0[n]$ using the chain rule, equation (2.14) is seen to be the Euler equation for a system of non-interacting electrons,

$$\left[-\frac{1}{2}\nabla^2 + v_{\mathrm{s}}[n](r,t)\right]\phi_i(t) = i\frac{\partial}{\partial t}\phi_i(t) \tag{2.15}$$

in the effective potential $v_{\mathrm{s}}[n](r,t)$, which depends itself on the density of the system

$$v_{\mathrm{s}}[n](r,t) = \int d^3r' \frac{n(r',t)}{|r-r'|} + v(r,t) + \frac{\delta A_{xc}[n]}{\delta n(r,t)}. \tag{2.16}$$

Equation (2.15) is the time-dependent Kohn-Sham equation. Given an initial set of Kohn-Sham orbitals $\phi_i(r,t_0)$, the time-dependent KS equation determines the time evolution of the density and consequently of all the physical observables.

2.2 Linear response in TD-DFT

Using the time-dependent Kohn-sham equation, we can calculate the response of a system to a time-dependent perturbation $v^{(1)}(r,t)$, which is switched on at time t_0. Since we need an initial state, we assume that the system is in its ground-state at time t_0, with ground-state Kohn-Sham orbitals $\phi_i^{(0)}(r)$ and the ground-state density $n^{(0)}(r)$. In this section, the development of Gross and Kohn [19] is followed.

We are interested in the linear response of the density $n^{(1)}(r,t)$, which is defined in terms of the non-interacting response function $\chi_{\rm s}(r,t;r',t')$ as

$$n^{(1)}(r,t) = \int d^3r' \int_{t_0}^{\infty} dt' \chi_{\rm s}(r,t;r',t') v_{\rm s}^{(1)}(r',t'). \tag{2.17}$$

The extended time-dependent potential $v_{\rm s}^{(1)}(r',t')$ includes the response of the effective potential (2.16) due to the response of the density. Thus $v_{\rm s}^{(1)}(r,t)$ is given by

$$v_{\rm s}^{(1)}(r,t) = v^{(1)}(r,t) + \int d^3r' \frac{n^{(1)}(r',t)}{|r-r'|} + \int d^3r' \int dt'\; f^{\rm xc}(r,t;r',t') n^{(1)}(r',t'), \tag{2.18}$$

where $f^{\rm xc}(r,t;r',t')$ is the exchange-correlation response kernel, defined as the functional derivative of the time-dependent exchange-correlation potential

$$f^{\rm xc}(r,t;r',t') = \left.\frac{\delta^2 A^{\rm xc}[n](r,t)}{\delta n(r,t)\delta n(r',t')}\right|_{n(r,t)=n^{(0)}(r)} = \left.\frac{\delta v^{\rm xc}[n](r,t)}{\delta n(r',t')}\right|_{n(r,t)=n^{(0)}(r)} \tag{2.19}$$

evaluated at the the ground-state density. [2]

[2] Until 1998, there was some doubt about the validity of this representation of $f^{\rm xc}(r,t;r',t')$. The, so-called causality problem is, that from causality of the response functions $\chi(r,t;r',t')$ and $\chi_{\rm s}(r,t;r',t')$ it is inferred that the exchange-correlation response kernel $f^{\rm xc}(r,t;r',t')$ is not symmetric under exchange of (r,t) and (r',t') and therefore cannot be the second functional derivative of $A^{\rm xc}[n]$. The issue was resolved by van Leeuwen [20] by defining a new action functional within the Keldysh formalism.

Equations (2.17) and (2.18) together constitute the time-dependent linear response equations which have to be solved self-consistently. Combining the two equations and taking the Fourier transform, we come to a single equation for the frequency-dependent linear response density $n^{(1)}(r,\omega)$

$$\int d^3r'\ \chi_{\rm s}(r,r';\omega)v^{(1)}(r',\omega) = \int d^3r''\left[\delta(r-r'') - \int d^3r'\ \chi_{\rm s}(r,r';\omega)\left\{\frac{1}{|r'-r''|} + f^{\rm xc}(r',r'';\omega)\right\}\right] n^{(1)}(r'',\omega). \tag{2.20}$$

The frequency-dependent response function $\chi_{\rm s}(r,r';\omega)$, calculated in [8] for example, is

$$\chi_{\rm s}(r,r';\omega) = \sum_{j,k}(f_k - f_j)\frac{\overline{\phi}_k^{(0)}(r)\phi_j^{(0)}(r)\overline{\phi}_j^{(0)}(r')\phi_k^{(0)}(r')}{\omega - (\epsilon_j - \epsilon_k) + i\delta}, \tag{2.21}$$

where f_j is the occupation number of the j-th orbital and δ is a small real constant to make the response function non-singular.

Equations (2.20) and (2.21) can now be used to compute the excitation energies of a system in its ground state. The idea is that the polarizability, and thus the linear response density $n^{(1)}$, has poles at the true excitation energies Ω. But the left hand side of (2.20) is in general finite as $\omega \to \Omega$. This means that the operator acting on $n^{(1)}(r,\omega)$ on the right hand side of (2.20) cannot be invertible for $\omega \to \Omega$. Therfore the true excitation energies are those, for which the operator on the right hand side of (2.20), acting on a response function $\zeta(r,\omega)$ is singular. In other words, we have to find the zero eigenvalues $\lambda(\omega) = 0$ of the following equation

$$\int d^3r'' \int d^3r' \chi_{\rm s}(r,r';\omega)\left\{\frac{1}{|r'-r''|} + f^{\rm xc}(r',r'';\omega)\right\}\zeta(r'',\omega) = \lambda(\omega)\zeta(r,\omega). \tag{2.22}$$

Note, that the quantity $\zeta(r,\omega)$ is not the response density $n^{(1)}(r,\omega)$, though in the literature the distinction is seldomly done.

2.3 TD-DFRT using perturbation theory

To give another point of view, and because its easier to derive equations in terms of response Kohn-Sham orbitals, we present an alternative derivation of the TD-DFRT equations using

perturbation theory. The formulation in terms of response orbitals has the advantage, that linear scaling techniques, especially the use of localised functions, can be applied. Of course, the equations derived here will be equivalent to equations constructed by using the formalism of the previous section 2.2.

As we have seen in section 2.1.1, we must start from an initial state, which is taken to be the ground-state calculated from

$$\hat{H}_\sigma^{(0)}(r)\phi_{j\sigma}^{(0)}(r) = \epsilon_{j\sigma}\phi_{j\sigma}^{(0)}(r). \tag{2.23}$$

Here, the $\phi_{j\sigma}^{(0)}(r)$ are the ground state orbitals and $\hat{H}_\sigma^{(0)}(r)$ is the unperturbed, ground-state Kohn-Sham Hamiltonian

$$\hat{H}_\sigma^{(0)}(r) = \left[-\frac{1}{2}\nabla^2 + v^{\text{ext}}(r) + \sum_{\tau=\alpha,\beta}\int d^3r' \frac{n_\tau^{(0)}(r')}{|r-r'|} + \frac{\delta E^{\text{xc}}[n]}{\delta n_\sigma(r)}\bigg|_{n^{(0)}(r)}\right], \tag{2.24}$$

where $v^{\text{ext}}(r)$ is the time-independent external potential containing of the electron-nuclei interaction. The ground state density is given by

$$n_\sigma^{(0)}(r) = \sum_j^{N_\sigma} \overline{\phi}_{j\sigma}^{(0)}(r)\phi_{j\sigma}^{(0)}(r) \tag{2.25}$$

We now consider a harmonic perturbation of frequency ω, as induced by an oscillating electric field (a photon)

$$\delta v(r,t) = \delta v^+(r)e^{+i\omega t} + \delta v^-(r)e^{-i\omega t}, \tag{2.26}$$

where δ is the perturbative parameter. This perturbation induces a response in the orbitals which can be expanded in orders of the perturbative parameter

$$\phi_{j\sigma}(r,t) = e^{-i\epsilon_{j\sigma}t}\sum_{m=0}^{\infty}\delta^m\phi_{j\sigma}^{(m)}(r,t). \tag{2.27}$$

In equation (2.27) we have extracted an overall time-dependent phase $e^{-i\epsilon_{j\sigma}t}$, equal to the phase in the ground-state. We already know the zeroth order term $\phi_{j\sigma}^{(0)}(r,t) = \phi_{j\sigma}^{(0)}(r)$. For the first order, linear response orbitals we use the ansatz

$$\phi_{j\sigma}^{(1)}(r,t) = \phi_{j\sigma}^{(+)}(r)e^{+i\omega t} + \phi_{j\sigma}^{(-)}(r)e^{-i\omega t}, \tag{2.28}$$

with the constraint that the only allowable response orbitals are linear combinations of the virtual orbitals of the ground-state calculation. This implies that the response orbitals are orthogonal to the ground-state orbitals, because they can be expanded in the basis of the Hilbert subspace complimentary to the ground-state orbital subspace. The condition can be imposed by choosing the gauge

$$\langle \phi_{i\sigma}^{(\pm)}(r) | \phi_{j\sigma}^{(0)}(r) \rangle = 0 \quad \text{for} \qquad \sigma = \alpha, \beta \quad \forall\, j = 0, \ldots, N_\sigma \quad \forall\, i = 1, \ldots, N_\sigma. \tag{2.29}$$

With this ansatz the linear response of the density becomes

$$\begin{aligned} n_\sigma^{(1)}(r,t) &= n_\sigma^{(+)}(r) e^{+i\omega t} + n_\sigma^{(-)}(r) e^{-i\omega t} \\ &= \sum_{j=0}^{N_\sigma} \left(\overline{\phi}_{j\sigma}^{(0)}(r) \phi_{j\sigma}^{(+)}(r) + \overline{\phi}_{j\sigma}^{(-)}(r) \phi_{j\sigma}^{(0)}(r) \right) e^{+i\omega t} + \\ &\qquad \left(\overline{\phi}_{j\sigma}^{(0)}(r) \phi_{j\sigma}^{(-)}(r) + \overline{\phi}_{j\sigma}^{(+)}(r) \phi_{j\sigma}^{(0)}(r) \right) e^{-i\omega t}. \end{aligned} \tag{2.30}$$

The response of the system provokes a change in the density dependent terms of the Hamiltonian leading to an effective perturbation for the positive and negative frequency parts

$$\begin{aligned} \delta v_\sigma^{\mathrm{eff}\pm}(r) &= \delta v^{\pm} + \delta v_\sigma^{\mathrm{SCF}\pm}(r) \\ &= \delta v^{\pm} + \delta \sum_{\tau=\alpha,\beta} \left[\int dr' \frac{n_\tau^{(\pm)}(r')}{|r - r'|} + \int dr' f_{\sigma,\tau}^{\mathrm{xc}}(r, r'; \pm\omega) n_\tau^{(\pm)}(r') \right]. \end{aligned} \tag{2.31}$$

$f_{\sigma,\tau}^{\mathrm{xc}}(r, r'; \pm\omega)$ is the Fourier transform of the exchange-correlation kernel already encountered in section 2.2.

Inserting (2.28) and (2.31) into (2.15), carrying out the derivatives and sorting according to positive and negative frequency parts leads to the two linear response equations in terms of the orbitals

$$\begin{aligned} &\left(\hat{H}_\sigma^{(0)}(r) - \epsilon_{j\sigma} \right) \phi_{j\sigma}^{(\pm)}(r) + \\ &\underbrace{\int dr' \left[\delta(r - r') + \sum_{k=0}^{N_\sigma} \phi_{k\sigma}^{(\pm)}(r) \overline{\phi}_{k\sigma}^{(0)}(r') \right]}_{Q_\sigma} \left\{ v^{\pm} + v_\sigma^{\mathrm{SCF}\pm}(r') \right\} \phi_{j\sigma}^{(0)}(r') = \mp\omega \phi_{j\sigma}^{(\pm)}(r). \end{aligned} \tag{2.32}$$

where the constraints (2.29) are accounted for by the projector Q_σ onto the virtual σ-spin subspace [3].

As already mentioned in the previous section 2.2, the linear response density has poles at the true excitation energies. As a consequence the operator acting on the linear response orbitals (everything in (2.32) except the $v^{\pm}\phi^{(0)}_{j\sigma}(r)$ term) must not be invertible, or in other words have zero eigenvalue, which leads to

$$\left(\hat{H}^{(0)}_\sigma(r) - \epsilon_{j\sigma}\right)\phi^{(\pm)}_{j\sigma}(r) + Q_\sigma v^{\mathrm{SCF}\pm}(r')\phi^{(0)}_{j\sigma}(r') = \mp\omega\phi^{(\pm)}_{j\sigma}(r). \tag{2.33}$$

The same remark as the one for (2.22) must be made here: The orbitals appearing in (2.33) are not the true linear response orbitals but some orbitals for which the operator has zero eigenvalue. But for lack of a better name, we shall continue to call them linear response orbitals.

Note that (2.33) is a set of coupled equations, since the linear response densities $n^{(\pm)}_\sigma(r)$ depend on both, positive and negative frequency, linear response orbitals. Therefore, the equations (2.33) are coupled trough $v^{\mathrm{SCF}\pm}(r')$, which depends on the linear response densities.

2.3.1 Tamm-Dancoff approximation

The Tamm-Dancoff approximation (TDA) [21] was introduced into the TD-DFRT formalism by Hirata and Head-Gordon [22]. It amounts to neglecting the occupied to virtual elements of the linear response density matrix, which corresponds to the neglect of the positive frequency linear response orbitals ($\phi^{(+)}_{j\sigma}(r) = 0$). This leads to computationally simpler equations

$$\left(\hat{H}^{(0)}_\sigma(r) - \epsilon_{j\sigma}\right)\phi^{(-)}_{j\sigma}(r) + Q_\sigma v^{\mathrm{SCF}-}(r)\phi^{(0)}_{j\sigma}(r) = \omega\phi^{(-)}_{j\sigma}(r). \tag{2.34}$$

Since the linear response density must be real, it has to be "symmetrized"

$$n^{(-)}_\sigma(r) = \frac{1}{2}\sum_{j=0}^{N_\sigma} \overline{\phi}^{(0)}_{j\sigma}(r)\phi^{(-)}_{j\sigma}(r) + \overline{\phi}^{(-)}_{j\sigma}(r)\phi^{(0)}_{j\sigma}(r). \tag{2.35}$$

The results in [22] show that the TDA yields excitation energies which are usually very close to those obtained using the full TD-DFRT equations. Differences are found for excited states having triplet near instability problems but for these excitations the TDA results are actually closer to the experimental excitation energies .

[3] It is easy to verify, that $\langle\phi^{(0)}_{i\sigma}|Q_\sigma|\psi\rangle = 0$ for $\forall\ 1 \le i \le N_\sigma$ and for all ψ.

2.3.2 Kohn-Sham excitation energies

If the linear response kernel is small compared to the first term on the left hand side in equation (2.33), then we can get approximate excitation energies by neglecting it altogether. The remaining equation

$$\left(\hat{H}_\sigma^{(0)}(r) - \epsilon_{j\sigma}\right) \phi_{j\sigma}^{(\pm)}(r) = \mp\omega\phi_{j\sigma}^{(\pm)}(r). \tag{2.36}$$

does no longer need to be evaluated self consistently and we can directly find the solutions by expanding the linear response orbitals in eigenvectors of the unperturbed Hamiltonian. The resulting excitation energies are given by the differences of virtual and occupied KS eigenvalues. In particular, the lowest excitation energy is $\omega = \epsilon^{\mathrm{LUMO}} - \epsilon^{\mathrm{HOMO}}$, since this is the smallest possible Kohn-Sham eigenvalue difference. The next higher excitation energy can either be the HOMO-1 to LUMO or the HOMO to LUMO+1 transition, whichever has the lower eigenvalue difference. This is the same excitation energy one would get by reducing the occupation number of a occupied Kohn-Sham orbital by one and adding one to the occupation number of a virtual Kohn-Sham orbital, keeping the density fixed, and then taking the difference with the ground-state energy. Therefore these excitation energies are also called Kohn-Sham excitation energies. Often the KS excitation energies are quite good approximations to the TD-DFRT excitation energies (as, for example, for the He atom) and sometimes they are not (for Be, for example). An explanation for this behavior is given in [23].

At any rate, the KS excitation energies can be used as an initial guess to the solution of the TD-DFRT equations as discussed in chapter 3.

2.4 Exchange-correlation functionals and kernel

Unfortunately, neither the exchange-correlation (XC) functional used in ground-state calculations $E^{\mathrm{xc}}[n]$, nor the XC action functional used in time-dependent calculations $A^{\mathrm{xc}}[n]$ are known exactly. In actual calculations they have to be approximated. For the sake of presenting a self-contained document, the next section 2.4.1 briefly discusses the XC functionals that were employed for the calculations shown in this work. Approximations to the XC action functional are discussed in section 2.4.2.

2.4.1 Exchange-correlation functionals

One important aspect of the Kohn-Sham theory is, that by separating out the independent-particle kinetic energy and the long-range Hartree term, the remaining XC energy can be well approximated by a *local* functional of the density

$$E^{\mathrm{xc}}[n_\alpha, n_\beta] \approx \int d^3r\, \varepsilon^{\mathrm{xc}}(n_\alpha(r), n_\beta(r)). \tag{2.37}$$

The simplest possible model for the electron density is that of a homogeneous electron gas, which means that the electronic density is constant over all space. The exchange energy can be given analytically in this case and its correlation energy has been calculated to great accuracy using quantum Monte-Carlo methods by Ceperley and Alder (CA) [24] and later by Ortiz and Ballone [25]. In order to use this correlation energy in DFT calculations, it has to be fitted to a functional of the density. The resulting approximation is called the local spin-density approximation (LSDA). Very popular parameterizations of the CA data are the one of Perdew and Zunger (PZ) [26] and of Vosko, Wilk and Nusair (VWN) [27]. Later, in 1992, Perdew and Wang (PW92) [28] gave yet another parameterization of the same data. Finally, in a paper on separable dual-space Gaussian pseudopotentials [29], Goedecker and coworkers presented a computationally convenient parameterization called the Padé (PADE) approximation, that closely reproduces the PW92 results and makes it very easy to calculate higher derivatives (needed in TD-DFT, see next section 2.4.2). Through their close relationship to the quantum Monte-Carlo data, the VWN and PADE functionals can be considered almost equal. This should be kept in mind when, later in this text, excitation energies obtained using these two functionals are compared.

To improve upon the LSDA, the inhomogeneous nature of the electron gas has to be taken into account. This has lead to the development of the generalized gradient approximation (GGA) functionals. Because these also take into account the gradient of the density, they are sometimes also called non-local or semi-local functionals, although they really are local, since they use only the gradient at the same point as the density. Out of the different proposals for the GGA exchange functional, the one of Becke given in 1988 (B88) [30] and the one of Perdew, Burke and Ernzerhof (PBE) [31] are of relevance in this work. The two agree quite well for small gradients, but differ for larger gradients. This is because they were designed for different purposes: The B88

was parameterized to give an asymptotically correct energy density and the PBE was designed for the simple, parameter-free form. Two important GGA correlation functionals are the one of Lee, Yang and Parr (LYP) [32] (often used together with B88, this is abbreviated BLYP) and the PBE correlation functional. The GGAs give a remarkable improvement for total energies and geometries in atomic and molecular systems, where the electron density differs quite strongly from the homogeneous gas. Using the GGAs DFT calculations have become more accurate, to the point of them being good enough for chemical applications.

2.4.2 XC kernel

The first time-dependent calculations of Zangwill and Soven [8] employed the adiabatic local density approximation (ALDA) for the XC action functional A^{xc}

$$A^{\mathrm{xc}}_{\mathrm{ALDA}}[n] \approx \int dt E^{\mathrm{xc}}_{\mathrm{LSDA}}[n]. \tag{2.38}$$

The ALDA is a special case of the adiabatic approximation which is local in time and thus doesn't allow for retardation effects.

$$f^{\mathrm{xc}}(r,t;r',t') \approx \delta(t-t')\left.\frac{\delta^2 E^{\mathrm{xc}}[n]}{\delta n(r,t)\delta n(r',t)}\right|_{n(r,t)=n^{(0)}(r,t)}. \tag{2.39}$$

Furthermore the adiabatic approximation is usually used together with a local XC functional to give the adiabatic and local approximation

$$f^{\mathrm{xc}}(r,t;r',t') \approx \delta(t-t')\left.\frac{\delta^2 E^{\mathrm{xc}}_{\mathrm{LSDA/GGA}}[n]}{\delta n(r,t)\delta n(r',t)}\right|_{n(r,t)=n^{(0)}(r,t)}. \tag{2.40}$$

In the ALDA, the XC functional is simply the LSDA XC functional.

As for the local and semi-local approximations to the XC energy functional, there's no physical justification for using these adiabatic and local approximations, except for the case of low frequencies and slowly varying densities. But its success in calculations give it somewhat legitimation.

The adiabatic and local approximation, and especially the ALDA, are the most widely used approximations, but, of course, efforts to find better approximations for the XC kernel are being made. In their paper of 1985, Gross and Kohn [33] derive an XC kernel functional, and the

properties thereof, based solely on the local approximation. Their, non-adiabatic, approximation includes a frequency-dependence of the XC kernel, but they find that it doesn't give significant improvements over the adiabatic approximation in the calculation of the photo-absorption spectra calculated done by Zangwill and Soven. In a later paper van Gisbergen *et al.* [34] investigate whether the frequency dependence of the XC kernel can improve the frequency dependence of the polarizabilities of atoms but find that this is not the case. Instead the frequency dependent XC kernel of Gross and Kohn over-corrects the frequency dependent polarizabilities. Therefore, the adiabatic approximation is still the workhorse of TD-DFRT calculations in atoms and molecules. In solids however, it is found the XC kernel must be non-local and frequency-dependent [35].

Chapter 3

Implementation with the Gaussian and plane waves (GPW) method

In the last chapter, approximations to exchange-correlation functionals were discussed. But to actually calculate anything using DFT, a computer executable implementation is needed and since computers don't have unlimited processing power and resources, further approximations have to be made. More specifically, the single-particle wavefunctions, or orbitals, which are vectors of an infinite-dimensional vector space, can only be represented by a finite number of parameters M in a computer program. This is usually done using a truncated expansion in a series of orthogonal, or non-orthogonal, basis functions $\{\varphi_\mu(r)\}$

$$\psi_i(r) = \sum_{\mu=1}^{M} c_{\mu i}(r)\varphi_\mu(r),$$

which leads to a formulation of the relevant equations in terms of matrices. Of course, matrices are ideally suited to be processed by computers. For the basis functions, Gaussian functions, plane waves and delta functions are the most common choices. Each of these have their own strengths and weaknesses.

Gaussian functions are localized in a region of space and are therefore best suited for wavefunctions that are localized, as are often encountered in atoms and in molecules. Because of their localized character, an efficient screening can be employed, which leads to sparse matrices.

This can be exploited to achieve linear scaling behavior, that means, an implementation, which has a computational cost that scales linearly with the system size. Because Gaussian functions are easy to handle, and there exist efficient analytic expressions [36] for all terms involved in quantum chemical and density functional calculations employing them, they have a tradition with quantum chemical codes and are widely used in molecular density functional codes.

Plane waves, on the other hand, are fully delocalized and have periodicity built in. They are therefore suited for delocalized orbitals, which appear in the valence and conduction bands of condensed matter. They make it hard to describe wavefunctions in the vicinity of atomic cores though, making it necessary to use a very large number of them and consequently requiring lots of memory. It's thus not surprising, that plane waves are widely used in band-structure calculations, often enhanced with some other method to treat the region of the atomic cores (known as the augmented plane waves (APW) method). Plane waves are closely connected to grid methods, since the plane waves correspond to grid-points in reciprocal space and it is possible to evaluate the Hartree term efficiently using plane waves and fast Fourier transforms (FFTs).

Finally, delta functions bring localization to the extreme and are equivalent to putting the wavefunctions on a grid in real space. They are the basis functions employed in fully numeric codes using finite difference schemes, where the kinetic energy operator is evaluated from a set of values of the orbitals on the grid.

The expansion of the wavefunctions in terms of M basis functions, instead of infinitely many ones, directly leads to another approximation in TD-DFRT. According to equation (2.21) the sum over all (infinitely many) virtual Kohn-Sham orbitals has to be taken, to find the excitation energies. But the ground-state Kohn-Sham matrix, calculated using the approximated wavefunctions, is of dimension $M \times M$ and has only M eigenvectors, or Kohn-Sham orbitals, and thus only $M - N$ virtual orbitals. This reduced subspace of virtual orbitals is an approximation, which has not been well studied. However, the number of basis functions has direct influence on the quality of the orbital themselves by governing the degrees of freedom available for optimization. It seems that this influence is much stronger than the one caused by the truncation of the subspace of virtual orbitals [37].

Therefore TD-DFRT calculations almost always use a large number of basis functions [1] so that the effect of this truncation of the virtual orbital subspace is probably not measurable.

In order to achieve a good computational performance, often further approximations are introduced. Very common is the fitting of the electronic density to a set of functions which usually differs from the set employed to represent the single-particle orbitals (see, for example [15, 38]). This method is called the auxiliary-function method, or the density-fitting method. The fitting functions are chosen for their mathematical properties, which can be used to speed up the calculation of the density dependent terms in the Kohn-Sham energy functional.

This chapter describes the implementation of the TD-DFRT equations in the framework of an existing Gaussians and Plane Waves (GPW) method computer program called CP2K [39]. The GPW method uses Gaussians for the expansion of the wavefunctions and uses planes wave as fitting functions for the density. Together with the use of pseudopotentials, this methods achieves a computational cost that scales linearly with the system size. A comprehensive discussion of this method and the implementation in CP2K is found in [40]. Here we will discuss the part of the GPW implementation concerning the TD-DFRT equations. The TDA was used rather than the full equations, since the TDA often yields better results for excitation energies and is considerably easier to implement. We do not present any source code, since the CP2K is open source software and the source code is therefore available to the interested reader from the Internet.

A somewhat similar method is presented in [41], though that method uses plane waves for the expansion of the orbitals as well. Therefore, it does not have an overlap matrix as the GPW method has.

3.1 Matrix formulation

Here and in the rest of the document, we restrict the discussion to real orbitals (functions of real numbers), a choice which is always possible in the absence of magnetic fields. As the name implies, the GPW method expands the Kohn-Sham orbitals in a set of M atom centered,

[1] Basis sets of triple zeta valence quality with polarization, and, in the case of atoms and molecules, diffuse functions, are recommended. For a review of basis sets see [2].

contracted Gaussian [2] basis functions $\varphi_\mu(r)$

$$\phi^{(0)}_{j\sigma}(r) = \sum_{\mu=1}^{M} c^{(0)}_{\mu j\sigma}\varphi_\mu(r) \tag{3.1}$$

$$\phi^{(\pm)}_{j\sigma}(r) = \sum_{\mu=1}^{M} c^{(\pm)}_{\mu j\sigma}\varphi_\mu(r). \tag{3.2}$$

$c^{(0)}_{\mu j\sigma}$ and $c^{(\pm)}_{\mu j\sigma}$ are the matrix elements of the ground-state coefficients matrix $c^{(0)}_\sigma$ and the linear response orbital matrices $c^{(\pm)}_\sigma$ respectively. The contracted Gaussians are not orthogonal and their scalar product defines the overlap matrix $\mathbf{S}$

$$\langle\varphi_\mu|\varphi_\nu\rangle = \mathbf{S}_{\mu\nu}. \tag{3.3}$$

Inserting the basis function expansions (3.1) and (3.2) into (2.34) and acting from the left with $\int d^3r\, \varphi_\mu(r)$ leads to the TD-DFRT matrix equations

$$\sum_{\nu=1}^{M}\left(\mathbf{F}_{\mu\nu\sigma}c^{(-)}_{\nu j\sigma} - \mathbf{S}_{\mu\nu}c^{(-)}_{\nu j\sigma}\epsilon_{j\sigma}\right) + \sum_{\nu=1}^{M}\underbrace{\sum_{\gamma=1}^{M}\left(\delta_{\mu\gamma} - \sum_{k=0}^{N_\sigma}\sum_{\delta=1}^{M}\mathbf{S}_{\mu\delta}c^{(0)}_{\delta k\sigma}c^{(0)}_{\gamma k\sigma}\right)}_{\mathbf{Q}_{\nu\gamma\sigma}}\mathbf{K}_{\gamma\nu\sigma}c^{(0)}_{\nu j\sigma} = \omega\sum_{\nu=1}^{M}\mathbf{S}_{\mu\nu}c^{(-)}_{\nu j\sigma}. \tag{3.4}$$

Here $\mathbf{Q}_{\nu\gamma\sigma}$ is a matrix element of the projector Q_σ and

$$\mathbf{F}_{\mu\nu\sigma} = \langle\varphi_\mu|\hat{H}^{(0)}_\sigma|\varphi_\nu\rangle \tag{3.5}$$

is the matrix of the ground-state Hamiltonian and

$$\begin{aligned}\mathbf{K}_{\mu\nu\sigma} &= \langle\varphi_\mu|\sum_{\tau=\alpha,\beta}\left[\mathbf{H}_\tau(r) + \mathbf{K}^{\mathrm{xc}}_{\sigma,\tau}(r)\right]|\varphi_\nu\rangle \\ &= \langle\varphi_\mu|\sum_{\tau=\alpha,\beta}\left[\int dr'\frac{n^{(-)}_\tau(r)}{|r-r'|} + \int dr' f^{\mathrm{xc}}_{\sigma,\tau}(r,r';\pm\omega)n^{(-)}_\tau(r')\right]|\varphi_\nu\rangle\end{aligned} \tag{3.6}$$

is the matrix of the TD-DFT kernel consisting of the Hartree part and the XC kernel.

[2] The contracted Gaussian functions are discussed in section 4.1.1

For a more compact notation, equation (3.4) is written in matrix form

$$\left(\mathbf{F}_\sigma c_\sigma^{(-)} - \mathbf{S}c_\sigma^{(-)}\mathcal{E}_\sigma\right) + (1 - \mathbf{SP}_\sigma)\,\mathbf{K}_\sigma c_\sigma^{(0)} = \omega \mathbf{S} c_\sigma^{(-)}, \tag{3.7}$$

where $\mathcal{E}_\sigma = \mathrm{diag}(\epsilon_{j\sigma})$ is the diagonal matrix of ground-state orbital eigenvalues and $\mathbf{P} = c_\sigma^{(0)} c_\sigma^{(0)^T}$ is the matrix of the electronic density in terms of contracted Gaussian basis functions. To see this, one simply inserts the expansions (3.1) into (2.13) and carries out the summation over the orbitals

$$n_\sigma^{(0)}(r) = \sum_{j=1}^{N_\sigma}\sum_{\mu=1}^{M} c_{\mu j\sigma}^{(0)}\varphi_\mu(r)\sum_{\nu=1}^{M} c_{\nu j\sigma}^{(0)}\varphi_\nu(r) = \sum_{\mu=1,\nu=1}^{M} \underbrace{\sum_{j=1}^{N_\sigma} c_{\mu j\sigma}^{(0)} c_{\nu j\sigma}^{(0)}}_{\mathbf{P}_{\mu\nu\sigma}} \varphi_\mu(r)\varphi_\nu(r) \tag{3.8}$$

Note that the eigenvalue equation (3.7) for the excitation energy ω has to be solved self-consistently, because the operator acting on the linear response orbitals depends on these orbitals itself.

3.1.1 Singlet and triplet excitation energies

In the case of spin-restricted ground-state system, we can calculate two types of electronic excitations: the ones that keep the spin of the excited electron the same, called *singlet* excitations (because the total spin wavefunction remains a singlet), and the ones which flip the spin of the excited electron, called triplet excitations (because the new total spin wavefunction belongs to a triplet). To distinguish between them, linear combinations of the response orbitals are formed.

$$u_{\mu j} = \frac{1}{\sqrt{2}}(c_{\mu j\alpha}^{(-)} + c_{\mu j\beta}^{(-)}) \tag{3.9}$$

is used for the singlets and

$$v_{\mu j} = \frac{1}{\sqrt{2}}(c_{\mu j\alpha}^{(-)} - c_{\mu j\beta}^{(-)}) \tag{3.10}$$

is used for the triplets. Inserting these into (3.7) and using the fact, that the XC kernel has spin symmetry, when evaluated for a spin-restricted ground-state density

$$f_{\alpha,\alpha}^{\mathrm{xc}} = f_{\beta,\beta}^{\mathrm{xc}} \tag{3.11}$$

$$f_{\alpha,\beta}^{\mathrm{xc}} = f_{\beta,\alpha}^{\mathrm{xc}}, \tag{3.12}$$

leads to two separate equations for singlets

$$(\mathbf{F}u - \mathbf{S}u\mathcal{E}) + (1 - \mathbf{SP})\left[2\mathbf{H}(r) + \mathbf{K}^{\mathrm{xc}}_{\alpha,\alpha}(r) + \mathbf{K}^{\mathrm{xc}}_{\alpha,\beta}(r)\right] c^{(0)} = \omega \mathbf{S}u, \tag{3.13}$$

and for triplets

$$(\mathbf{F}v - \mathbf{S}v\mathcal{E}) + (1 - \mathbf{SP})\left[\mathbf{K}^{\mathrm{xc}}_{\alpha,\alpha}(r) - \mathbf{K}^{\mathrm{xc}}_{\alpha,\beta}(r)\right] c^{(0)} = \omega \mathbf{S}v. \tag{3.14}$$

Note that the spin indices have been omitted for all quantities but for the XC kernel, because these quantities are identical for up and down spin-densities in the restricted case.

3.2 Density representation

In the eigenvalue equations for the excitation energies (3.7), (3.13) and (3.14) we have two densities appearing. First, there is the ground-state density $n^{(0)}_\sigma(r)$ given by (2.25), which appears in the ground-state calculation and in the XC kernel. Second, there is the linear response density $n^{(-)}_\sigma(r)$, given by (2.35), which only appears in the XC kernel. Both these densities are defined in terms of double sums over the basis functions as in (3.8). This representation of the density, however, makes the calculation of the Hartree part and the XC potential and kernel very expensive (scaling as $\mathcal{O}(N^4)$ and $\mathcal{O}(N^3)$ respectively).

To efficiently evaluate the terms depending on these densities the GPW method uses a PW representation of these densities. We will proceed to show this for a general density $n(r)$.

The expansion of the density in terms of PW is given by

$$n(r) = \frac{1}{\Omega} \sum_G n(G) e^{iG\cdot r}, \tag{3.15}$$

where Ω is the volume of the unit cell, G are reciprocal lattice vectors, and $n(G)$ are the expansion coefficients for the PW representation. This PW representation of the density is in principle exact, but in actual calculations the expansion has to be truncated at certain cutoff value G_C, including all G vectors for which $|G| < G_C$. This means that accuracy of the PW representation is conveniently controlled using just one parameter, the cutoff energy E_C

$$E_C = \frac{1}{2} G_C^2. \tag{3.16}$$

The included G vectors define a real-space grid in the unit cell and the $n(G)$ are related to the values of $n(r)$ on this real-space grid by Fourier transformation. Therefore the plane wave expansion is easily obtained by first mapping the density onto the real-space grid and then using a Fast Fourier transformation. The evaluation on the real-space grid can be done very efficiently by exploiting the local nature of the Gaussian functions trough screening.

Using the convolution theorem (a convolution becomes a multiplication when using a Fourier transform) it is possible to evaluate the Hartree potential on the real-space grid efficiently

$$\int dr' \, \frac{n(r')}{|r - r'|} \quad \rightarrow \quad \sum_G \frac{n(G)}{G^2}. \tag{3.17}$$

The local XC potential can be evaluated on the real-space grid directly. The integration onto the Kohn-Sham matrix can again be screened efficiently, so that the overall complexity of the code goes linearly with the system size ($\mathcal{O}(N)$), rather than cubically ($\mathcal{O}(N^3)$) as would be the case using conventional density fitting methods.

3.3 Technical details

As mentioned before, the excitation energy equations (3.7), or (3.13) and (3.14) have to be solved self-consistently because the operator acting on the linear response orbitals depends itself on these orbitals. These equations can be thought of as eigenvalue equations of the form

$$Ax_i = \omega_i S x_i, \tag{3.18}$$

where A is the operator on the left hand side of the equations (3.7), (3.13), or (3.14), acting on the linear response orbitals denoted by x_i, and the eigenvalues ω_i are the excitation energies we seek. In the Gaussian basis formulation the matrix to be diagonalized, corresponding to the operator A, is of dimension $(NM \times NM)$, where N is the number of occupied orbitals and M the number of basis functions. But usually, one is interested in only the lowest few (say 10) excitation energies. Fully diagonalizing the problem would therefore be a waste of CPU and memory resources. Iterative subspace eigensolvers allow the computation of a few extremal (smallest or largest) eigenvalues and, using appropriate transformations, even internal eigenvalues of a matrix can be calculated. They achieve this by constructing a set of trial vectors,

which are used to approximate the desired eigenvectors. Starting from a small set of trial vectors, new vectors are added in iterations until the target accuracy of the approximation is reached. The number of required trial vectors is typically small compared to the dimension of the matrix. Moreover it's not necessary to know the matrix to be diagonalized explicitly. Instead only the product of the matrix with a trial vector must be computed. This is an considerable benefit, since the matrix in question can be too large to fit into the available computer memory, and it allows to take advantage of the sparsity of the matrix.

3.3.1 Iterative subspace eigensolver

The Lanczos algorithm [42] and the Davidson [43] algorithm were implemented in the TD-DFRT code reported in this work. They share the same basic structure and can be implemented using the same subroutine. The basic structure is as follows:

```
starting from initial trial vectors {q_i}
repeat:
   calculate b_i = A q_i
   calculate T_ij = q_i^T b_j
   diagonalize T → ε̃
   add new vectors q_{i+n}
   reorthogonalize the vectors {q_i}
until convergence of ε̃
```

The true eigenvalues of the matrix A are approximated by the eigenvalues $\tilde{\varepsilon}$ of the much smaller matrix T. The approximation is good, if the eigenvectors we are looking for can be well approximated by the subspace $\{q_i\}$. The algorithm convergences monotonically towards the eigenvalues of A (see [42] for a discussion of the convergence behavior). The two, Lanczos and Davidson, differ in the way, how the new vectors to be added are chosen.

The Lanczos algorithm adds one vector at a time according to the power method. The vector to be added is just the last vector, that was added, multiplied by A and then orthogonalized

to the other trial vectors. In this way the subspace vectors $\{q_i\}$ resemble a power series of A applied to the initial q_0 vector $\{q_0, Aq_0, A^2q_0, \ldots\}$.

The standard Davidson algorithm also adds one vector at a time. If we have M subspace vectors $\{q_i\}$, which result in the approximate eigenvalues $\lambda_i^{(M)}$ and eigenvectors $\alpha_i^{(M)}$, then the new vector is the residuum of the desired eigenvalue k

$$r = \sum_{i=1}^{M} \alpha_{k,i}^{(M)} \left[(Aq_i) - \lambda_k^{(M)} (Sq_i) \right], \tag{3.19}$$

where $\alpha_{k,i}^{(M)}$ is the i-th component of the k-th eigenvector in the M-th iteration. Again, this vector has to be orthogonalized to the other trial vectors already at hand. By adding not just one residuum but the residua to several desired eigenvalues, it is possible to extend the algorithm to allow the addition of several vectors. This, so-called, Block-Davidson algorithm is widely used in quantum chemistry codes.

Preconditioner

The convergence behavior of the Davidson algorithm can be improved by using a preconditioner on the residuum

$$d_{,i} = (\lambda_k^{(M)} S_{ii} - A_{ii})^{-1} r_{,i}. \tag{3.20}$$

In our case, we do not know the A matrix explicitly, but for the purpose of preconditioning, the diagonal may be approximated by the operator without the LR kernel, which are just the KS excitation energies as discussed in section 2.3.2. The first few of these are available from the initial guess (see next section) and for the remaining we can just take the highest KS excitation energy computed in the initial guess plus a constant. This preconditioner assumes that the matrix A is sparse and almost diagonal. In the test calculations, however, it did not give a significant improvement of the convergence and the result presented in this work were computed without the use of the preconditioner.

Initial guess

The iterative eigensolvers just described are very sensitive to the initial guess. This means that the number of iterations depends strongly on the quality of the initial trial vector given. Therefore we want the best possible initial guess for the TD-DFRT calculation. Section 2.3.2 already mentioned, that the Kohn-Sham excitation energies are often good approximations to the TD-DFRT eigenvalues. This means, that we can find the guess to the j-th excitation energy by first finding the a and k indices for which the Kohn-Sham excitation energy $\epsilon_a - \epsilon_k$ is the j-th smallest, and then construct the corresponding linear response orbitals. It follows, that these orbitals are given by setting all the linear response orbitals to zero except the k-th one, which is set equal to the a-th virtual orbital.

If we want to compute the first n eigenvalues of a system, the initial guess should include n vectors. Thus n virtual orbitals are needed to generate the initial guess.

An alternative way to calculate the initial guess is to solve (2.36) to find the Kohn-Sham excitations energy solutions, instead of constructing them explicitly. Again, only the first n of these solutions are of interest and therefore an iterative subspace eigensolver can be used to find them. In CP2k the same iterative eigensolver routine is used to solve the TD-DFRT equations and generate the Kohn-Sham excitations initial guess. Because the eigensolver does not need the matrix itself, but just the result of the matrix-vector multiplication, it is possible to control the type of operator applied, full TD-DFRT or Kohn-Sham excitation type, by passing a parameter to the routine. The Kohn-Sham excitations problem is computationally much less expensive and the time needed to generate the initial guess in this way is negligible compared to the time needed to solve the eigenvalue equation with the full response kernel.

In the CP2K program both ways to compute the initial guess, construction and solution of the Kohn-Sham excitation equation, are combined. The user input includes a `LUMOS N` keyword, which causes the computation of `N` virtual orbitals. These are then used as initial guess for the determination of the Kohn-Sham excitations. Finally, the Kohn-Sham excitations are used as the initial guess for the TD-DFRT equations.

3.3.2 Calculation of the kernel

The Hartree part of the response kernel can be calculated using the same techniques as for the Hartree term in the ground-state calculation, discussed in section 3.2. In doing so, the linear response density is mapped on the real-space grid corresponding to the plane wave basis for the density.

Because the exchange-correlation kernel is local in space the detour trough reciprocal space is not necessary and the evaluation can be done on the real-space grid directly. In the adiabatic approximation the XC kernel becomes the second partial derivative of the one-particle exchange-correlation density. Using the rules of functional derivation (see Appendix A) we find for the ALDA, where $E^{\mathrm{xc}}_{\mathrm{LDA}}$ depends only on the (spin-)density,

$$\int dr\, \frac{\delta^2 E^{\mathrm{xc}}_{\mathrm{LDA}}[n]}{\delta n_\sigma(r)\delta n_\tau(r)}\bigg|_{n=n^{(0)}} n_\tau^{(-)}(r) = \frac{\partial^2 e^{\mathrm{xc}}_{\mathrm{LDA}}[n]}{\partial n_\sigma(r)\partial n_\tau(r)}\bigg|_{n=n^{(0)}} n_\tau^{(-)}(r). \tag{3.21}$$

For spin-unrestricted GGA the exchange-correlation functionals can depend on up to 5 variables: The spin-up and spin-down densities n_α and n_β, the norm of the gradient of the spin-densities $|\nabla n_\alpha|$ and $|\nabla n_\beta|$, and the norm of the gradient of the total density $|\nabla n|$.[3] These 5 variables can be combined in 15 different ways for the second derivatives of the one-particle exchange-correlation energy density. In the CP2K program, the full analytic second functional derivatives are implemented. The calculation of the second functional derivative is demonstrated in appendix A. Equation (A.7) shows the most general case.

In the adiabatic and local approximation (section 2.4.2), the expression for the singlet excitations (3.13) can be simplified further by using the fact, that $\mathbf{K}^{\mathrm{xc}}_{\alpha,\alpha}(r)+\mathbf{K}^{\mathrm{xc}}_{\alpha,\beta}(r) = 2\mathbf{K}^{\mathrm{xc}}(r)$, where $\mathbf{K}^{\mathrm{xc}}(r)$ is the XC kernel evaluated using the restricted densities. The resulting equation

$$(\mathbf{F}u - \mathbf{S}u\mathcal{E}) + (1 - \mathbf{SP})\, 2\, [\mathbf{H}(r) + \mathbf{K}^{\mathrm{xc}}(r)]\, c^{(0)} = \omega \mathbf{S}u. \tag{3.22}$$

reduces the number of second derivatives to 6 possibilities.

[3] Sometimes this variable is replaced by the scalar product of the gradient of the spin-densities $\nabla n_\alpha \cdot \nabla n_\beta$. However, note that

$$\frac{\partial}{\partial(\nabla n_\alpha \cdot \nabla n_\beta)} = \frac{1}{|\nabla n|}\frac{\partial}{\partial|\nabla n|}.$$

3.4 Test calculations

To validate the TD-DFRT implementation, excitation energies of a set of small test molecules in gas phase were calculated using the PBE and the PADE exchange-correlation functionals. These are compared to excitation energies obtained by other TD-DFRT codes, namely the Turbomole code [44] with the PBE functional and the ADF package (see references in [45]) with the LDA functional, with values given in [45] and [46]. Six of the test molecules, have a spin-unpolarized ground-state wavefunction, and thus singlet and triplet energies were calculated: nitrogen (N_2), carbon monoxide (CO), water (H_2O), ethylene (C_2H_4), formaldehyde (CH_2O), and acetone ($CO(CH_3)_2$). The geometries of the first five of these are taken form [22]. The geometry of acetone cannot be found in that paper. It is determined by geometry optimization using the CPMD program package [47], with the PBE functional, a cubic cell of 14Å and a plane wave cutoff of 110 Ry. The ADF values are not obtained at the same geometry as the values calculated with the GPW method. Four more test molecules, beryllium hydrate (BeH), beryllium fluoride (BeF), CH_3, and cyanide (CN), which have a spin-polarized ground state wavefunction and require a spin unrestricted calculation, were also calculated. The geometries of these are taken from [48]. For convenience, the geometries are summarized in table 3.1.

Experimental excitation energies are form [49] for N_2, from [50] for CO, from [22] for H_2O, from [51] for C_2H_4, from [52] for CH_2O, from [48] for the spin-polarized molecules BeH, BeF, CH_3, and CN. The first singlet and the first two triplet experimental excitation energies of $CO(CH_3)_2$ are from [53]. The second to fourth singlet excitation energies acetone are from [54]. Because there's some ambiguity concerning the experimental singlet excitation energies of formaldehyde, and [45] follows [55], which does not give the higher lying R A_2 and R B_2 excitation energies, the ADF excitation energies of these two excitations in formaldehyde are lacking. Also, triplet excitation energies for water and acetone using ADF are not presented.

3.4.1 Computational details

It is known, that large basis sets containing polarization and diffuse functions are important for excited-state calculations in gas phase. For calculations in CP2K a Dunning [56, 57] basis set of quadruple zeta quality, that is adapted to the Goedecker-Teter-Hutter pseudopotentials

Molecule	Geometry	Point group
N_2	$r_{N\text{-}N} = 1.0977$Å	$\mathcal{D}_{\infty h}$
CO	$r_{C\text{-}O} = 1.1283$Å	$\mathcal{C}_{\infty v}$
H_2O	$r_{O\text{-}H} = 0.9584$Å, $\angle_{H\text{-}O\text{-}H} = 104.45°$	$\mathcal{C}_{2v}$
C_2H_4	$r_{C\text{-}C} = 1.3349$Å, $r_{C\text{-}H} = 1.0848$Å, $\angle_{C\text{-}C\text{-}H} = 121.70°$	$\mathcal{D}_{2h}$
CH_2O	$r_{C\text{-}O} = 1.2200$Å, $r_{C\text{-}H} = 1.1039$Å, $\angle_{H\text{-}C\text{-}O} = 122.19°$	$\mathcal{C}_{2v}$
$CO(CH_3)_2$	$r_{C_1\text{-}O} = 1.2212$Å, $r_{C_1\text{-}C_2} = 1.5158$Å, $\angle_{O\text{-}C_1\text{-}C_2} = 121.69°$,	$\mathcal{C}_{2v}$
	$r_{C_2\text{-}H_1} = 1.0947$Å, $\angle_{C_1\text{-}C_2\text{-}H_1} = 110.16°$, $\angle_{0\text{-}C_1\text{-}C_2\text{-}H_1} = 0°$,	
	$r_{C_2\text{-}H_2} = 1.1005$Å, $\angle_{C_1\text{-}C_2\text{-}H_2} = 110.30°$, $\angle_{0\text{-}C_1\text{-}C_2\text{-}H_2} = 121.30°$,	
	$r_{C_2\text{-}H_3} = 1.1005$Å, $\angle_{C_1\text{-}C_2\text{-}H_3} = 110.30°$, $\angle_{0\text{-}C_1\text{-}C_2\text{-}H_3} = -121.30°$	
BeH	$r_{Be\text{-}H} = 1.339$Å	$\mathcal{C}_{\infty v}$
BeF	$r_{Be\text{-}F} = 1.355$Å	$\mathcal{C}_{\infty v}$
CH_3	$r_{C\text{-}H} = 1.069$Å, $\angle_{H\text{-}C\text{-}H} = 120°$	$\mathcal{D}_{3h}$
CN	$r_{C\text{-}N} = 1.128$Å	$\mathcal{C}_{\infty v}$

Table 3.1: Molecular geometries of the molecules that were calculated in this work. See text for references. Note that in acetone, due to symmetry, there are two topologically different types of C atoms, labeled C_1 and C_2, and 3 types of H atoms, labeled H_1, H_2 and H_3.

[29, 58] according to [40], is used. The basis is augmented with 3 polarization functions for each atom. Furthermore, for all involved atomic species, except beryllium, a diffuse function is added for every angular momentum shell present in the basis. A cubic box of 20 Å and density cutoff energy of 400 Ry is used. The excitation energies are converged to the fifth significant digital.

3.4.2 Analysis

The results of the calculations are given in tables 3.2 and 3.3. The average of the absolute deviations (AAD) of Turbomole/PBE with experiment, GPW/PBE with experiment, GPW/PADE with experiment, and finally Turbomole/PBE with GPW/PBE are given in table 3.4 in units of electronvolts. The excitations are labeled V or R, for valence or Rydberg. Valence excitations are excitations to valence orbitals. Accordingly Rydberg excitations, are excitations into Rydberg orbitals, which are usually quite extended. See appendix C for an exact definition of the

Molecule	State	TM/PBE	CP2K/PBE	CP2K/PADE	ADF	Exp
N_2	$V^1\ \Pi_g$	9.103	9.295	9.221	9.07	9.31
	$V^1\ \Sigma_u^-$	9.682	9.688	9.687	9.68	9.92
	$V^1\ \Delta_u$	10.081	10.197	10.198	10.23	10.27
	$V^3\ \Sigma_u^+$	7.530	7.704	7.610	7.90	7.75
	$V^3\ \Pi_g$	7.400	7.945	7.922	7.58	8.04
	$V^3\ \Delta_u$	8.290	8.836	8.824	8.84	8.88
CO	$V^1\ \Pi$	8.235	8.535	8.430	8.17	8.51
	$V^1\ \Sigma^-$	9.853	9.861	9.876	9.87	9.88
	$V^1\ \Delta$	10.173	10.276	10.295	9.19	10.23
	$V^3\ \Pi$	5.729	6.173	5.989	5.96	6.32
	$V^3\ \Sigma^+$	8.101	8.413	8.400	8.41	8.51
	$V^3\ \Delta$	8.715	9.160	9.160	9.18	9.36
	$V^3\ \Sigma^-$	9.853	9.861	9.876	9.87	9.88
H_2O	$R^1\ B_1$	6.409	6.378	6.556	9.47	7.4
	$R^1\ A_2$	7.669	7.669	7.865	11.4	9.1
	$R^1\ A_1$	8.550	8.511	8.610	11.6	9.7
	$R^1\ B_1$	8.869	8.952	9.166	16.4	10.0
	$R^1\ A_1$	9.499	9.344	9.590	17.5	10.17
	$R^3\ B_1$	6.070	6.124	6.278		7.2
C_2H_4	$R^1\ B_{3u}$	6.469	6.427	6.632	6.59	7.11
	$V^1\ B_{1u}$	7.359	7.724	7.834	7.36	7.60
	$R^1\ B_{1g}$	7.018	6.940	7.172	7.03	7.80
	$R^1\ B_{2g}$	6.972	6.972	7.160	7.02	8.01
	$R^1\ A_g$	7.790	7.683	7.921	7.28	8.29
	$R^1\ B_{3u}$	8.150	8.147	8.337	7.31	8.62
	$V^3\ B_{1u}$	4.224	4.719	4.687	4.63	4.36
	$R^3\ B_{3u}$	6.351	6.378	6.572	6.55	6.98
	$R^3\ B_{1g}$	6.934	6.958	6.971	7.03	7.79
	$R^3\ B_{2g}$	6.892	6.892	7.107	7.00	7.79
	$R^3\ A_g$	7.490	7.520	7.751	7.26	8.15
CH_2O	$V^1\ A_2$	3.713	3.777	3.637	3.69	4.07
	$R^1\ B_2$	5.781	5.757	5.900	5.85	7.11
	$R^1\ B_2$	6.796	6.752	6.892	6.57	7.97
	$R^1\ A_1$	6.543	6.519	6.663	6.54	8.14
	$R^1\ A_2$	7.186	7.112	7.264		8.37
	$R^1\ B_2$	8.009	8.036	8.113		8.88
CH_2O	$V^3\ A_2$	2.959	3.150	3.002	3.08	3.50
	$V^3\ A_1$	5.536	6.045	6.025	6.20	5.86
	$R^3\ B_2$	5.626	5.703	5.832	5.79	6.83
	$R^3\ B_2$	6.674	6.700	6.831	6.61	7.79
	$R^3\ A_1$	6.431	6.497	6.630	6.58	7.91
$CO(CH_3)_2$	$V^1\ A_2$	4.177	4.239	4.190	4.17	4.35
	$R^1\ B_2$	4.963	4.956	5.095	5.47	6.34
	$R^1\ A_2$	5.958	5.951	6.122	6.99	7.36
	$R^1\ A_1$	5.773	5.779	5.956	6.81	7.40
	$R^1\ B_2$	6.112	6.101	6.300	7.33	7.45
	$V^3\ A_2$	3.550	3.706	3.654		4.16
	$V^3\ A_1$	5.640	5.691	5.865		5.88

Table 3.2: Calculated and experimental excitation energies, in electronvolts, of six molecules with an spin-unpolarized ground-state wavefunction. Geometries are given in table 3.1. See text for references to the experimental values.

Molecule	State	TM/PBE	CP2K/PBE	CP2K/PADE	Exp.
BeH	V Π	2.484	2.644	2.407	2.48
	R Π	5.511	5.908	5.750	6.32
BeF	V Π	4.081	4.242	4.132	4.14
	R Σ^+	5.651	5.602	5.624	6.16
	R Σ^+	6.657	6.484	6.591	6.27
CN	V Π	1.707	2.089	1.685	1.32
	V Σ^+	3.105	3.678	3.296	3.22
CH_3	R A_1'	4.933	4.900	5.006	5.73
	R A_2''	6.328	6.266	6.461	7.44

Table 3.3: Calculated and experimental excitation energies, in electronvolts, of the test molecules with a polarized ground-state wavefunction. Geometries are given in table 3.1. See text for references to the experimental values.

	TM/PBE - Exp.	CP2K/PBE - Exp.	CP2K/PADE - Exp.	TM/PBE - CP2K/PBE
V	0.292 ± 0.210	0.184 ± 0.180	0.174 ± 0.154	0.255 ± 0.192
R	1.01 ± 0.345	1.03 ± 0.361	0.860 ± 0.339	0.0556 ± 0.0750

Table 3.4: Average absolute deviations of the methods and experiment and standard deviation thereof in electronvolts

Rydberg excitations. Looking at the deviation of the GPW implementation with Turbomole we see that there is an excellent agreement for the Rydberg states: the AAD of only 0.0556 eV is well below the benchmark accuracy in TD-DFRT, which is 0.1 eV. For the valence states, we see that there is a significant deviation, of 0.255 eV, of the GPW results from the results obtained with Turbomole. But looking at the deviations of the two programs from experiment, it is noted that CP2K is doing significantly better (0.180 eV) for valence states than Turbomole (0.292 eV). It has previously been observed [22], that the Tamm-Dancoff approximation gives very similar results to the full TD-DFRT equations for Rydberg states but can give different results for valence states. This mainly occurs in systems that have the triplet near instability problem. For these states, the Tamm-Dancoff is observed to give better results than the full

TD-DFRT equations. The GPW results are in agreement with this and we can conclude that the deviations of the values obtained with CP2K from those obtained with Turbomole are due to the Tamm-Dancoff approximation.

Looking at the performance of the LDA versus the PBE, it can be said, that the GGA does not give a significant improvement compared to the LDA. For the valence excitations the GGA, with an AAD of 0.180 eV, and the LDA, with an AAD of 0.174 eV, have essentially the same performance. But for the Rydberg excitations the LDA, with an AAD of ≈ 0.860 eV, is doing better than the GGA, with 1.03 eV. This is consistent with the expected performance of the GGAs in TD-DFRT. Since the GGAs mainly improve the XC potential shape in the proximity of the atomic core (in the high density, and high gradient region), the Rydberg states are not expected to improve by using the GGA. Note that we only test the PBE GGA functional. Other GGA can give different results, maybe even performing slightly better than the LDA, but the trend is the same for all standard GGAs though.

The LDA values obtained from the ADF program are not calculated at the same geometries as the Turbomole or CP2K values and different basis sets are used as well. They are given here to show that other TD-DFRT codes give similar results as the Turbomole and the CP2K programs. The singlet excitation energies of water and acetone are the exception to this trend. These were calculated with a basis set lacking diffuse functions. The effect of this on the Rydberg excitations is clearly demonstrated in acetone. While the valence A_2 excitation agrees reasonably well with the CP2K PADE value, the Rydberg excitations are significantly higher than the CP2K PADE values. This is because the Rydberg orbitals are poorly represented by using a basis set that lacks diffuse functions.

Chapter 4

Implementation with the Gaussian and augmented plane waves (GAPW) method

The plane waves used to expand the density in the GPW method, as discussed in the previous chapter, are the solutions to the one-particle Schrödinger equation with a constant potential V

$$\left(-\frac{1}{2}\nabla^2 + V\right) e^{-ikr} = Ee^{-ikr}, \tag{4.1}$$

and with

$$|k| = \sqrt{2(E-V)}. \tag{4.2}$$

This means that a linear combination of plane waves is appropriate to appromixate the wavefunction of a particle moving in a nearly constant potential. Such potentials occur for the valence electrons in solids, which is why the plane waves are a popular choice for the basis functions in DFT codes aimed at solids. However, if the potential is far from constant and the wavefunctions are no longer very smooth, then the plane waves become less suited and one has to use additional techniques to be able to do the calculation economically.

If we want to apply this reasoning to the approximation of the electronic density by plane waves, we have to consider, that the density is the sum of the amplitude squared of the electron orbitals.

Thus there are regions where the density is smooth, because the potential, that the electrons see in these regions, is varying slowly and the density is mostly given by the valence orbitals. On the other hand, there are regions, near the atomic cores, where the density is fluctuating strongly, because the potential in these regions, the Coulombic attraction of the nucleus, is varying strongly. Figures 4.1 and 4.2 illustrate this for the case of a formaldehyde molecule.

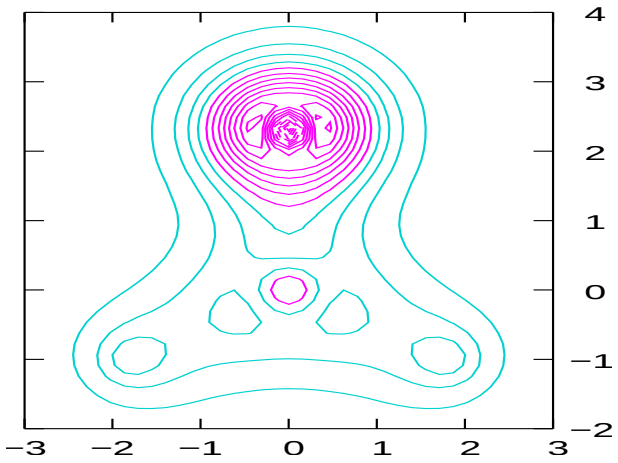

Figure 4.1: Contour plot a the ground-state density of formaldehyde (calculated using pseudopotentials), in the plane of the molecule. Axis ticks are given in atomic units.

The technique that is used in CP2K, and many other programs, to be able to use plane waves, are the pseudopotentials. The idea is to replace the strong Coulomb attraction and the strongly localized core electrons by an effective potential, called pseudopotential, that acts on the valence electrons. The calculation using pseudopotentials consequently only treats the orbitals of the valence electrons and the density becomes smooth and therefore expandable in a manageable number of plane waves. Basically the orbitals of the core electrons are fixed, or frozen, in a pseudopotential calculation. Typically, this has no effect on the quality of the calculated properties, since the core electrons generally do not affect the investigated phenomena, for example the bonds between atoms or the conduction bands of solids. However, there are some properties, for example NMR chemical shifts, for which the core states play an important role. Furthermore, calculations including heavy atoms, which means atoms from the third row and down in the periodic table, still require a very large number of plane waves, because the density is fluctuating strongly in the vicinity of the atomic cores, even when using pseudopotentials.

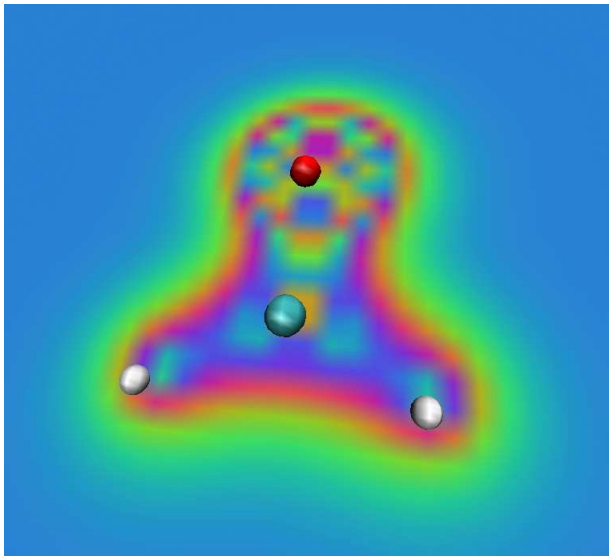

Figure 4.2: Color representation of one slice of the electronic ground-state density of a formaldehyde molecule (oxygen in red, carbon is blue, and the hydrogens are white), calculated with the CP2K program. The rapid changing of the colors near the oxygen atom illustrates the strong fluctuations of the density near the atomic cores very well.

In order to address these issues Lippert *et. al.* [59] proposed the Gaussian and augmented plane waves (GAPW) method, which is based, in part, on the projector augmented waves (PAW) method of Blöchl [60]. In addition to the plane waves, the GAPW method uses strongly localized Gaussian functions to represent the density, which results in a reduction of the number of plane waves necessary to accurately approximate the density. The next section 4.1 gives a brief discussion of the GAPW formalism. A more complete presentation of the method applied to pseudopotential calculation can be found in [59] and the GAPW method for all-electron systems, including the core electrons, is discussed in [61] and [62].

4.1 The GAPW method

The idea of the GAPW method is to use two different sets of fitting functions for the electron density. Near the atomic cores, which is where the density is fluctuating strongly, drawn in magenta in figure 4.1, localized Gaussian functions are used. These densities near the cores are

the hard densities $n_A(r)$, where the index A denotes a nucleus. In the region outside the atomic regions, the so-called interstitial region, which also contains the chemical bonds, the density is smooth and is expanded in plane waves. The resulting density is the soft density $\tilde{n}(r)$. Up to here, this scheme is similar to the augmented plane waves (APW) method, which is widely used in band-structure calculations. But contrary to the APW method, in the GAPW method, the densities are not cut and matched at the boundaries of the regions. Instead, the hard and the soft densities are extended over all space and soft compensation densities $\tilde{n}_A(r)$ are defined, which exactly cancel the contributions of the hard densities in the interstitial region and the contributions of the soft density in the atomic regions.

Thus the density is partitioned in the following way

$$n(r) = \tilde{n}(r) + \sum_A n_A(r) - \sum_A \tilde{n}_A(r), \tag{4.3}$$

where the sums run over all atomic cores denoted by A.

Let U_A be the atomic region around atom A. It does not overlap with any other atomic region U_B. The interstitial region is denoted by I. Then it is assumed that the overall smooth density $\tilde{n}(r)$ and the atom centered soft density $\tilde{n}_A(r)$ cancel in the atomic region

$$\tilde{n}(r) - \tilde{n}_A(r) = 0 \quad \text{for} \quad r \in U_A. \tag{4.4}$$

Furthermore, the hard and soft atom centered densities are assumed to cancel in the region outside U_A

$$n_A(r) - \tilde{n}_A(r) = 0 \quad \text{for} \quad r \notin U_A. \tag{4.5}$$

Lastly, we assume, that the exact density $n(r)$ is equal to the overall soft density $\tilde{n}(r)$ in the interstitial region

$$n(r) - \tilde{n}(r) = 0 \quad \text{for} \quad r \in I. \tag{4.6}$$

These assumptions make sure, that (4.3) holds for all space, and this can now be exploited to calculate the Hartree and XC terms independently for the soft $\tilde{n}(r)$ and atom centered hard $n_A(r)$ and soft $\tilde{n}_A(r)$ parts of the density.

The evaluation of the semi-local XC functionals, like the LDA and GGA's, is straightforward. Using the new partitioning, the XC energy functional reads

$$E^{\text{xc}}[n] = E^{\text{xc}}[\tilde{n}] + \sum_A E^{\text{xc}}[n_A] - \sum_A E^{\text{xc}}[\tilde{n}_A]. \tag{4.7}$$

The first term, employing the plane wave soft density, can be evaluated in exactly the same way as in the GPW method (chapter 3). The other terms, using the atom centered densities expanded in Gaussians, can be accurately evaluated using atomic grids.

The non-local Hartree energy functional, however, is more difficult and requires the introduction of screening densities

$$n^0(r) = \sum_A n_A^0(r) = \sum_{lm} Q_A^{l,m,A} g_A^{lm}(r) \tag{4.8}$$

$$\tilde{n}^0(r) = \sum_A \tilde{n}_A^0(r) = \sum_{l,m,A} Q_A^{lm} \tilde{g}_A^{lm}(r) \tag{4.9}$$

that are expanded in hard $g_A^{lm}(r)$ and soft $\tilde{g}_A^{lm}(r)$ Gaussians, respectively. Hard and soft refers to the magnitude of the exponent of the Gaussian, as explained in section 4.1.1.

The Q_A^{lm} are defined as

$$Q_A^{lm} = N q^{lm}[n_A - \tilde{n}_A + n_A^Z], \tag{4.10}$$

where $q^{lm}[n]$ is the multipole moment operator, n_A^Z is the charge density of the ionic core at atom A, and N is a normalization constant. These screening densities exactly cancel the electrostatic multipole moments of the one-center densities and thus allow a separation of the contributions to the Hartree energy. As a result the Hartree energy can be written as

$$\begin{aligned} E^{\text{H}}[n + n^Z] =& E^{\text{H}}[\tilde{n} + \tilde{n}^0] + \sum_A \left\{ E^{\text{H}}[n_A + n_A^Z] - E^{\text{H}}[\tilde{n}_A + n_A^0] \right\} \\ &+ E^{\text{H}}[n^0] - E^{\text{H}}[\tilde{n}^0] + \int dr\; v^{\text{H}}[n^0 - \tilde{n}^0]\tilde{n}, \end{aligned} \tag{4.11}$$

where

$$E^{\text{H}}[n] = \frac{1}{2} \iint dr dr' \frac{n(r)n(r')}{|r - r'|} \tag{4.12}$$

and

$$v^{\mathrm{H}}[n](r) = \int dr \frac{n(r')}{|r - r'|}. \tag{4.13}$$

The first term in (4.11) is global and can be evaluated in the PW representation. The other terms are local one-, two-, and three-center integrals and can be evaluated either analytically, using recursion relations [36], or on atom centered meshes. The current CP2K implementation uses the analytic evaluation.

4.1.1 Construction of the density

The total electronic density

$$n(r) = \sum_{\mu\nu} P_{\mu\nu}\varphi_\mu(r)\varphi_\nu(r). \tag{4.14}$$

is given by its expansion in terms of atomic basis functions $\varphi_\mu(r)$, which in turn are linear combinations of primitive Cartesian Gaussian functions $g_{a_i}^{l,m}(r; R_A)$

$$g_{\alpha_i}^{l,m}(r; R_A) = x^{l_x} y^{l_y} z^{l_z} e^{-\alpha_i (r-R_A)^2} \quad \text{with} \quad l_x + l_y + l_z = l. \tag{4.15}$$

The Cartesian Gaussians have an angular momentum with quantum number l and magnetic quantum number m. The value of m is determined by the choice of l_x, l_y and l_z which are natural numbers. For the discussion of the construction of the GAPW densities, only the exponent α_i matters and we map all the indices of $g_{a_i}^{l,m}(r; R_A)$ onto a single index i

$$g_i(r) \propto e^{-\alpha_i (r-R_i)^2}, \tag{4.16}$$

where R_i now is the position of the atomic core on which the Cartesian Gaussian $g_i(r)$ is centered. Therefore we define the contraction coefficients $C_{i\mu}$ by writing the basis functions $\varphi_\mu(r)$ as

$$\varphi_\mu(r) = \sum_i C_{i\mu} g_i(r) \tag{4.17}$$

Here the sum runs over all primitive Gaussian functions present in the calculation.

Soft density

Using Cartesian Gaussians, the strong variations of the density are modeled via functions with a large exponent α_i. We can therfore construct soft atomic basis functions $\tilde{\varphi}_\mu(r)$ by omitting from the contraction (4.17) those Gaussians with an exponent α_i larger than a threshold value T, thus defining new contraction coefficients $\tilde{C}_{i\mu}$

$$\tilde{\varphi}_\mu(r) = \sum_i \tilde{C}_{i\mu} g_i(r) \tag{4.18}$$

where

$$\tilde{C}_{i\mu} = 0 \qquad \text{for} \quad \alpha_i > T \tag{4.19}$$

$$\tilde{C}_{i\mu} = C_{i\mu} \qquad \text{for} \quad \alpha_i \leq T. \tag{4.20}$$

The threshold value T is chosen such that the Gaussians with an exponent larger than T are contained in the atomic region U_A of the atom on which they are centered. In this sense, the adjective "hard" is used for quantities that may contain all the Gaussian functions, whereas "soft" is used for quantities that are made up Gaussians with an exponent smaller than T. Figure 4.1.1 shows a sketch of a hard and its softened Gaussian function.

Summing the density matrix $P_{\mu\nu}$ with the new soft basis leads to the soft density

$$\tilde{n}(r) = \sum_{\mu\nu} P_{\mu\nu} \tilde{\varphi}_\mu(r) \tilde{\varphi}_\nu(r). \tag{4.21}$$

It follows from the construction of the soft basis functions $\tilde{\varphi}_\mu(r)$, that the soft density fulfills the requirement (4.6) and that the size of the atomic regions govern the number of primitive Gaussians that remain the in the expansion of the soft density. Like in the GPW case, the soft density is then mapped onto the real-space grid and Fourier transformed into reciprocal space to calculate the XC and Hartree terms

$$\tilde{n}(r) = \frac{1}{\Omega} \sum_G \tilde{n}(G) e^{iG \cdot r}. \tag{4.22}$$

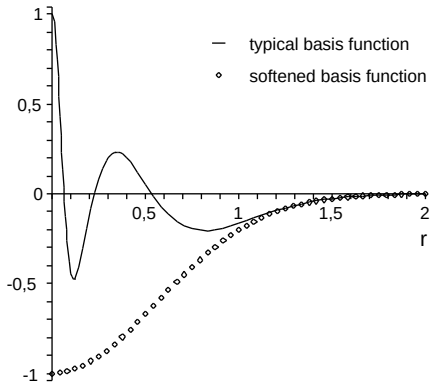

Figure 4.3: Sketch of a hard Gaussian (solid line) and the corresponding softened Gaussian (diamonds) basis function in arbitrary units. Only the radial component is shown. The basis function is centered on $r = 0$ in this case.

Atom centered densities

The atom centered densities $n_A(r)$ and $\tilde{n}_A(r)$ are expanded in the primitive Gaussians that are available from the basis functions and which are centered on the respective atom. This ensures a linear scaling performance of the method, since the number of primitive Gaussians localized on a single atom is independent of the system size. To this end we find new contraction coefficients $C'_{i\mu}$ and $\tilde{C}'_{i\mu}$ which build a new hard $\{\chi_\mu\}$ and soft basis $\{\tilde{\chi}_\mu\}$. The basis vectors χ_μ and $\tilde{\chi}_\mu$ belonging to atom A include the primitive Gaussians, that are centered on the atom itself (only the soft ones in the case of the soft $\tilde{\chi}_\mu$). They also include the projection, onto the primitive Gaussians centered on A, of the tails of those basis functions φ_μ which are not centered on A, and which reach into the atomic region of A (again only the soft ones for the soft basis).

We will now show how to obtain the hard density n_A centered on atom A. If φ_μ is centered on the current atom, then we can use that function directly

$$\chi_\mu = \varphi_\mu, \tag{4.23}$$

so that

$$C'_{i\mu} = C_{i\mu} \qquad \text{for } \varphi_\mu \text{ centered on atom } A. \tag{4.24}$$

But if the basis function φ_μ is centered on another atom than A, then only its tail will reach into the atomic region U_A and we are looking for the function χ_μ with

$$\varphi_\mu(r) \approx \chi_\mu(r) = \sum_{i \in A} C'_{i\mu} g_i(r) \qquad \text{for} \quad r \in U_A. \tag{4.25}$$

For this we define a number of projectors consisting of primitive Gaussians $p_i(r) \propto \exp(-a_i(r - R_A)^2)$ equal to the number of primitive Gaussians $g_i(r)$ centered on the atom A. The exponents of the projectors are chosen according to a geometric progression $a_i = 2a_{i-1}$ with the smallest exponent such that the corresponding projector function is confined in the region U_A. The projectors can be used to compute the $C'_{i\mu}$ by

$$\langle p_b | \varphi_\mu \rangle = \sum_{i \in A} C'_{i\mu} \langle p_b | g_i \rangle \tag{4.26}$$

or

$$C'_{i\mu} = \sum_j \langle p | g \rangle^{-1}_{ij} \langle p_j | \varphi_\mu \rangle. \tag{4.27}$$

The hard atom centered density $n_A(r)$ can now be written using the $C'_{i\mu}$ coefficients

$$n_A(r) = \sum_{i,j \in A} \sum_{\mu\nu} C'_{i\mu} P_{\mu\nu} C'_{j\nu} g_i(r) g_j(r). \tag{4.28}$$

The soft atom centered density $\tilde{n}_A(r)$ can in principle be constructed in the same way but since the hard and soft atom centered densities from the atoms other than A coincide by requirement (4.5) we can use the same coefficients for the basis functions not centered on A

$$\tilde{C}'_{i\mu} = C'_{i\mu} \qquad \text{for} \quad \mu \notin A. \tag{4.29}$$

If the basis function $\tilde{\varphi}_\mu$ is centered on A we can again directly use the coefficients of that basis function

$$\tilde{C}'_{i\mu} = \tilde{C}_{i\mu} \qquad \text{for} \quad \mu \in A. \tag{4.30}$$

Now we also have the expansion of the soft atom centered density $\tilde{n}_A$

$$\tilde{n}_A(r) = \sum_{i,j \in A} \sum_{\mu\nu} \tilde{C}'_{i\mu} P_{\mu\nu} \tilde{C}'_{j\nu} g_i(r) g_j(r). \tag{4.31}$$

It has to be noted, that the atomic regions U_A are only used as a helping construct to create the coefficient matrices $\tilde{C}$, C' and $\tilde{C}'$. Therefore they do not explicitly appear in the final GAPW representation of the density, but are hidden in the localization requirements for the basis functions. Furthermore, the coefficient matrices $\tilde{C}$, C' and $\tilde{C}'$ have to be determined only once for the whole self-consistent cycle calculation.

4.2 TD-DFRT using GAPW

In this section we will look at the combination of TD-DFRT with the GAPW method. The TD-DRFT equations (3.7), (3.13), and (3.14) are written as matrix equations in terms of atomic basis functions and there are two densities involved. First, there is the ground-state density $n_\sigma^{(0)}(r)$, resulting from a ground-state calculation with the Kohn-Sham matrix $\mathbf{F}_\sigma$. Secondly, to compute the linear response kernel the linear response density $n_\sigma^{(-)}(r)$ and the ground-state density are required.

To do a GAPW TD-DFRT calculation we do a GAPW ground-state calculation and apply the same partitioning as in the ground-state calculation to the linear response density. Therefore we use the same contraction coefficient matrices with the linear response density matrix $P_{\mu\nu}^{(-)}$

$$\tilde{n}^{(-)}(r) = \sum_{\mu\nu} P_{\mu\nu}^{(-)} \tilde{\varphi}_\mu(r) \tilde{\varphi}_\nu(r) \tag{4.32}$$

$$n_A^{(-)}(r) = \sum_{ab\in A} \sum_{\mu\nu} C'_{a\mu} P_{\mu\nu}^{(-)} C'_{b\nu} g_a(r) g_b(r) \tag{4.33}$$

$$\tilde{n}_A^{(-)}(r) = \sum_{ab\in A} \sum_{\mu\nu} \tilde{C}'_{a\mu} P_{\mu\nu}^{(-)} \tilde{C}'_{b\nu} g_a(r) g_b(r) \tag{4.34}$$

The Hartree term in the linear response kernel has the same form as the Hartree term for the ground-state calculation, except that it is evaluated using the linear response density. This means that it can be calculated using the same formula (4.11), even the same program subroutines, as in the ground-state calculation, by substituting the linear response density matrix $P_\sigma^{(-)}$ for the ground-state matrix $P_\sigma^{(0)}$. In addition, in the program code, we have to temporarily set the charge distribution of the ionic cores n_A^Z to zero for the purpose of calculating the Hartree contribution of the linear response density, since their contribution is not needed in the calculation of the linear response kernel.

It's not possible to give a GAPW expression for a general, possibly non-local, XC kernel, but for the adiabatic and local approximation (section 2.4.2) this can be done. In this approximation we have to multiply a local function of the density by the linear response density

$$\int dr\, \left.\frac{\delta^2 E^{\mathrm{xc}}[n]}{\delta n_\sigma(r)\delta n_\tau(r)}\right|_{n=n^{(0)}} n^{(-)}(r) = \int dr\, \left.\frac{\delta^2 E^{\mathrm{xc}}[n]}{\delta n_\sigma(r)\delta n_\tau(r)}\right|_{n=\tilde{n}^{(0)}+\sum_A n_A^{(0)}-\sum_A \tilde{n}_A^{(0)}} \{\tilde{n}^{(-)}(r) + \sum_B n_B^{(-)}(r) - \sum_B \tilde{n}_B^{(-)}(r)\}. \tag{4.35}$$

This could lead to cross terms between the overall soft and the atom centered parts of the two involved densities. But due to the local nature of XC functionals employed and because the same GAPW partitioning is used for the densities, all these cross terms cancel and we are left with terms to be evaluated on the same regions, or density parts,

$$\int dr\, \left.\frac{\delta^2 E^{\mathrm{xc}}[n]}{\delta n_\sigma(r)\delta n_\tau(r)}\right|_{n=n^{(0)}} n^{(-)}(r) = \int dr\, \left.\frac{\delta^2 E^{\mathrm{xc}}[n]}{\delta n_\sigma(r)\delta n_\tau(r)}\right|_{n=\tilde{n}^{(0)}} \tilde{n}^{(-)}(r) + \sum_A \left.\frac{\delta^2 E^{\mathrm{xc}}[n]}{\delta n_\sigma(r)\delta n_\tau(r)}\right|_{n=n_A^{(0)}} n_A^{(-)}(r) - \sum_A \left.\frac{\delta^2 E^{\mathrm{xc}}[n]}{\delta n_\sigma(r)\delta n_\tau(r)}\right|_{n=\tilde{n}_A^{(0)}} \tilde{n}_A^{(-)}(r). \tag{4.36}$$

The calculation leading to this result is carried out in appendix B. In the CP2K implementation all the terms of (4.36) are evaluated on a real-space grid and then integrated onto the Kohn-Sham matrix utilizing the screening of the Gaussian functions. This way, the computational cost to calculate the linear response operator scales linearly with the system size.

4.3 Test calculations

4.3.1 Convergence with plane wave cutoff

The convergence, with respect to the plane wave cutoff parameter E_C, of the GAPW method for ground-state calculations has previously been investigated [59, 62]. It was found, that the energies and geometries of single molecules are well converged with a modest cutoff of about 200 Ry. Here the convergence of the excitation energies with respect to the plane wave cutoff shall be discussed.

The convergence behavior of the first 3 singlet excitation energies of N_2 is plotted in figure 4.4. The shape of the curves may suggest that the excitation energies are not well converged, but

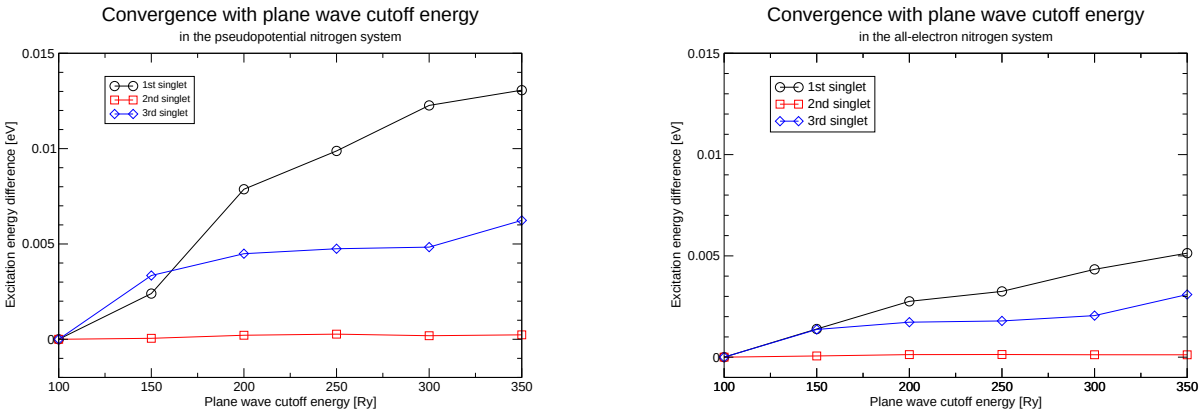

Figure 4.4: Excitation energy differences, relative to the result at 100 Ry cutoff, of the first 3 singlet excitations of N_2. Left panel shows the pseudopotential calculation and right panel the all-electron calculation.

a look on the energy scale reveals, that the worst converged excitation energy (the 1st singlet exciation energy in the pseudopotential calculation) is converged to less than 0.01 eV at 200 Ry. Again this is well below the benchmark accuracy of 0.1 eV. This shows, that a GAPW TD-DFRT can, as anticipated, give converged results with a smaller number of plane waves compared to the GPW method.

4.3.2 Small molecules

The same small molecules as in chapter 3 were tested with the GAPW method. Both, pseudopotential, as well as all-electron calculations were done. The same periodic cell is used in all cases. The GAPW pseudopotential calculation employs the same pseudopotentials and basis sets as the GPW calculation. The all-electron calculations are done using a quadruple zeta quality basis set of Dunning [56] augmented, except for Beryllium, with diffuse functions. The PBE XC functional was used for all GAPW calculations and the plane wave cutoff energy was set to 250 Ry in all cases. The results are summarized in tables 4.1 and 4.2, where the pseudopotential and all-electron results are marked with a "/pseudo." and "/all-elec." appended respectively. The tables also show the GPW PBE values from the previous chapter 3 for comparison.

In general it can be said, that the GAPW method agrees very well with the GPW method.

Molecule	State	TM	GPW/pseudo.	GAPW/pseudo.	GAPW/all-elec.	Exp.
N_2	$V^1\ \Pi_g$	9.103	9.295	9.332	9.276	9.31
	$V^1\ \Sigma_u^-$	9.682	9.688	9.689	9.683	9.92
	$V^1\ \Delta_u$	10.081	10.197	10.267	10.257	10.27
	$V^3\ \Sigma_u^+$	7.530	7.704	7.737	7.711	7.75
	$V^3\ \Pi_g$	7.400	7.945	8.089	8.113	8.04
	$V^3\ \Delta_u$	8.290	8.836	8.904	8.904	8.88
CO	$V^1\ \Pi$	8.235	8.535	8.568	8.510	8.51
	$V^1\ \Sigma^-$	9.853	9.861	9.850	9.858	9.88
	$V^1\ \Delta$	10.173	10.276	10.431	10.451	10.23
	$V^3\ \Pi$	5.729	6.173	6.180	6.188	6.32
	$V^3\ \Sigma^+$	8.101	8.413	8.759	8.837	8.51
	$V^3\ \Delta$	8.715	9.160	9.321	9.366	9.36
	$V^3\ \Sigma^-$	9.853	9.861	9.849	9.857	9.88
H_2O	$R^1\ B_1$	6.409	6.378	6.398	6.419	7.4
	$R^1\ A_2$	7.669	7.669	7.696	7.682	9.1
	$R^1\ A_1$	8.550	8.511	8.521	8.557	9.7
	$R^1\ B_1$	8.869	8.952	8.983	8.882	10.0
	$R^1\ A_1$	9.499	9.344	9.377	9.555	10.17
	$R^3\ B_1$	6.070	6.124	6.148	6.190	7.2
C_2H_4	$R^1\ B_{3u}$	6.469	6.427	6.428	6.449	7.11
	$V^1\ B_{1u}$	7.359	7.724	7.735	7.755	7.60
	$R^1\ B_{1g}$	7.018	6.972	6.974	7.002	7.80
	$R^1\ B_{2g}$	6.972	6.940	6.940	6.958	8.01
	$R^1\ A_g$	7.790	7.776	7.688	7.755	8.29
	$R^1\ B_{3u}$	8.150	8.147	8.148	8.141	8.62
	$V^3\ B_{1u}$	4.224	4.719	4.773	4.805	4.36
	$R^3\ B_{3u}$	6.351	6.378	6.378	6.405	6.98
	$R^3\ B_{1g}$	6.934	6.958	6.962	6.991	7.79
	$R^3\ B_{2g}$	6.892	6.892	6.892	6.916	7.79
	$R^3\ A_g$	7.490	7.520	7.526	7.616	8.15
CH_2O	$V^1\ A_2$	3.713	3.777	3.885	3.873	4.07
	$R^1\ B_2$	5.781	5.757	5.775	5.771	7.11
	$R^1\ B_2$	6.796	6.752	6.766	6.793	7.97
	$R^1\ A_1$	6.543	6.519	6.537	6.533	8.14
	$R^1\ A_2$	7.186	7.112	7.127	7.191	8.37
	$R^1\ B_2$	8.009	8.036	8.052	7.989	8.88
	$V^3\ A_2$	2.959	3.150	3.263	3.262	3.50
	$V^3\ A_1$	5.536	6.045	6.323	6.379	5.86
	$R^3\ B_2$	5.626	5.703	5.719	5.719	6.83
	$R^3\ B_2$	6.674	6.700	6.717	6.742	7.79
	$R^3\ A_1$	6.431	6.497	6.515	6.513	7.91
$CO(CH_3)_2$	$V^1\ A_2$	4.177	4.239	4.332	4.326	4.35
	$R^1\ B_2$	4.963	4.956	4.966	4.969	6.34
	$R^1\ A_2$	5.958	5.951	5.968	5.967	7.36
	$R^1\ A_1$	5.773	5.779	5.857	5.884	7.40
	$R^1\ B_2$	6.112	6.101	6.125	6.121	7.45
	$V^3\ A_2$	3.550	3.706	3.796	3.798	4.16
	$V^3\ A_1$	5.640	5.691	5.709	5.710	5.88

Table 4.1: Calculated and experimental excitation energies, in electronvolts, of the six molecules mentioned in the text, with an unpolarized ground-state wavefunction. See text for the calculation parameters and the references of the experimental values.

Molecule	State	TM	GPW/pseudo.	GAPW/pseudo.	GAPW/all-elec.	Exp.
BeH	V Π	2.484	2.644	2.640	2.613	2.48
	R Π	5.511	5.908	5.914	5.854	6.32
BeF	V Π	4.081	4.242	4.244	4.195	4.14
	R Σ^+	5.651	5.602	5.599	5.623	6.16
	R Σ^+	6.657	6.484	6.482	6.523	6.27
CN	V Π	1.707	2.089	2.114	1.851	1.32
	V Σ^+	3.105	3.678	3.698	3.529	3.22
CH_3	R A_1'	4.933	4.900	4.893	4.795	5.73
	R A_2''	6.328	6.266	6.256	6.228	7.44

Table 4.2: Calculated and experimental excitation energies, in electronvolts, of the four molecules mentioned in the text, with a polarized ground-state wavefunction. See text for the calculation parameters and the references of the experimental values.

GPW/pseudo. - GAPW/pseudo.	GPW/pseudo. - GAPW/all-elec.
0.0428 ± 0.0659	0.0685 ± 0.0820

Table 4.3: Average absolute deviations of the GAPW method from the GPW method and standard deviation thereof in electronvolts

Table 4.3 shows the AADs of the GAPW method using pseudopotentials and all-electrons from the GPW method using pseudopotentials. In both cases the AAD is well below 0.1 eV with the ADD of the all electron implementation being slightly larger. This small deviation of the GAPW results from the GPW results comes from the slightly different accuracy in the density representation of the two methods. Through its use of well-adapted fitting functions near the nuclear cores, the GAPW typically achieves a more accurate representation of the density at comparable computational cost than the GPW method.

We conclude that the combination of TD-DFRT with the GAPW method is a reliable and efficient implementation to compute excitation energies within the TD-DFRT formalism.

Chapter 5

Improving the excitation energies

As soon as the molecular formulation of TD-DFRT was completed [15, 63] a number of implementations appeared [64, 65, 38, 66, 67, 68, 22, 69] presenting the calculation of response properties of such molecular systems. It was soon found [68, 22], that TD-DFRT can give superior results to Hartree-Fock based single-excitation theories such as configuration interaction singles (CIS) and random phase approximation (RPA) at a roughly comparable computational cost. In particular it was found that valence excitations, that is excitations into valence orbitals, are very good [64, 65, 38, 70, 68] while Rydberg transitions are generally not so well represented [66, 67]. Interestingly this trend is independent from the XC functional used. Contrary to total energy and geometry calculations, the GGAs do not improve the approximate excitation energy of the Rydberg states. All this is corroborated by the results presented in chapter 3 and 4.

To see why standard XC functionals fail to give reasonable results for Rydberg excitations, we have to turn to the XC potential in section 5.1.

5.1 The importance of the exchange-correlation potential

In section 2.3.2, we have seen, that the so called KS excitation energies are often good approximations to the TD-DFRT excitation energies. But even when they are not, these KS excitation energies still make up a large portion of the TD-DFRT excitation energy. The KS excitation

energies are determined by the ground state calculation and this means mainly by the XC potential employed in the ground state calculation (assuming the calculation is well converged with respect to the basis set, and the density approximation employed). This suggests, that the XC potential plays a big role in the calculation of TD-DFRT excitation energies. In fact several papers [34, 37] argue that the XC potential is the most important approximation in a TD-DFRT calculation.

Generally it is found that, using standard XC potentials (from LDA and GGA's), the few lowest lying excitation energies are often quite good, while the higher lying ones are usually several electronvolts too small. The accepted explanation for this behavior [71, 37] is that an error cancellation occurs for the excitations which are of valence character. These are excitations to orbitals which are localized in the same region of space as the occupied orbitals. Hence the orbitals excited from and excited to see the same domain of the XC potential and a possible error in the potential cancels out. But this error cancellation does not happen for the Rydberg excitations, where the virtual orbitals do not share the same region of space as the valence orbitals and hence see a different, possibly incorrect, potential. Furthermore, it is found, that the XC potential employed in the ground-state calculation has the largest impact on the absolute position of the excitation energies [34, 37]. Therefore the inaccurate XC potentials are responsible for the bad estimations of the Rydberg excitation energies.

There are two important problems with the standard XC potentials: the derivative discontinuity (DD) and the self-interaction error (SIE).

In a paper of 1982, Perdew and Levy [72] show that, if the number of electrons N is allowed to change and take on non-integer values, the XC potential should exhibit a discontinuity as N increases trough an integer value. From this they deduce the asymptotic behavior of the XC potential

$$\lim_{r\to\infty} \frac{\delta E^{\mathrm{xc}}}{\delta n} = \lim_{r\to\infty} v^{\mathrm{xc}}(r) \geq 0. \tag{5.1}$$

Later, the same authors, together with Sahni, [73] find that the exact XC potential must vanish asymptotically and that the eigenvalue of the HOMO ϵ^{HOMO} is equal to minus the first ionization potential (IP) I of the system

$$\epsilon^{\mathrm{HOMO}} = -I. \tag{5.2}$$

This is the generalization of Koopmans' theorem to DFT. The same result is also found independently by Almbladh and von Barth [74], who furthermore show that, for the exact XC potential, the eigenvalue of the HOMO is governed by the asymptotic behavior of the XC potential, which must asymptotically vanish as $-1/r$

$$\lim_{r\to\infty} v^{\mathrm{xc}}(r) = -\frac{1}{r}. \tag{5.3}$$

The integer discontinuity is not taken into account by the presently used standard LDA and GGA functional, which are continuous in the number of electrons. Therefore they do not exhibit the correct asymptotic behavior. Instead they vanish too rapidly in the asymptotic region. As a result, the orbital eigenvalues of the outer orbitals are too large (not negative enough) by several electronvolts. It is thus the asymptotic region of the XC potential that is mainly responsible for the bad estimates of Rydberg excitation energies in TD-DFRT calculations using standard XC functionals [71]. Note however, that some standard XC potentials, and some of the proposed improved potentials presented below, do not even vanish asymptotically, nor do they need to do so for the purpose of calculating TD-DFRT excitation energies: The addition of a constant to the XC potential does not have any influence on the calculated excitation energies because its effect is a uniform shift of all orbital eigenvalues and only eigenvalue differences enter the TD-DFRT equations. Only the shape of the XC potential is important for the excitation energies and that means that an $-(1/r)$ behavior is needed in the asymptotic region.

As mentioned before in section 2.4.1, the separation of the Hartree energy is one of the strong points of the Kohn-Sham formalism, since it allows, together with the functional for the kinetic energy of the non-interacting particles, to find good approximations to the remaining XC energy. On the other hand this Hartree term now also poses a problem because it includes the Coulomb energy of the electrons with themselves. In Hartree-Fock theory, this self-interaction (SI) is canceled by an exchange term, but in the Kohn-Sham DFT formalism, with the local XC functionals, it is not. Naturally, some efforts to improve the Kohn-Sham method try to include a self-interaction correction (SIC) in the XC functionals. The hybrid functionals [75, 76], like B3LYP and PBE0, which include a fraction of the Hartree-Fock exchange, are very successful in the quantum chemistry community. The use of hybrid functionals has a striking effect on calculated excitation energies (see, for example, [77]), providing a kind of average between Hartree-Fock and GGA DFT excitation energies. Another proposal, by Iikura *et. al.* [78], is to

use HF exchange only asymptotically, that means only from a certain distance from the atomic cores. This leaves the short ranged correlation of DFT intact and only corrects where it is necessary. They report much improved excitation energies for systems where the occupied orbital excited from and the virtual orbital excited to are widely separated (so-called charge transfer excitations). However, these theories that include Hartree-Fock exchange are no longer purely density functional theories, making them computationally more expensive.

Since it is easier to model the XC potential directly than the XC functional, several proposals to improve the XC potential were made recently. In the following we discuss some of these.

The idea to use orbital dependent functionals $E^{\mathrm{xc}}[\phi_i[n]]$ goes back to a paper of 1953 by Sharp and Horton [79]. This developed into the optimized effective potential (OEP) method [80, 81]. To find the XC potential corresponding to an orbital dependent functionals, the chain-rule has to be used

$$v^{\mathrm{xc}}(r) = \frac{\delta E^{\mathrm{xc}}[\phi_i[n]]}{\delta n(r)} = \sum_i \int \frac{\delta E^{\mathrm{xc}}}{\delta \phi_i(r')} \frac{\delta \phi_i(r')}{\delta v^{\mathrm{s}}(r'')} \frac{\delta v^{\mathrm{s}}(r'')}{\delta n(r)} dr' dr'' \tag{5.4}$$

Here the $\phi_i(r)$ are the orbitals and $v^{\mathrm{s}}(r)$ is the total effective potential of the non-interacting system. The first term $\delta E^{\mathrm{xc}}/\delta\phi_i(r')$ on the right hand side of (5.4) can be written as a non-local potential $v^{\mathrm{xc}}_{\mathrm{NL},i}(r')$ times $\phi_i(r')$, the second term $\delta\phi_i(r')/\delta v^{\mathrm{s}}(r'')$ can be evaluated using perturbation theory to

$$\frac{\delta \phi_i(r')}{\delta v^{\mathrm{s}}(r'')} = G_0(r', r'')\phi_i(r''), \tag{5.5}$$

where $G_0(r', r'')$ is the Greens function for the non-interacting system. The third term is just an inverse of the response function χ similar to the one we have already encountered in section 2.2. Multiplying by this χ, multiplying from the right with $\phi_i(r)$, and integrating, we find an integral equation for the XC potential $v^{\mathrm{xc}}(r)$

$$\sum_i \int dr' \phi_i(r') \left[v^{\mathrm{xc}}(r') - v^{\mathrm{s}}(r') \right] G_0(r', r)\phi_i(r) = 0. \tag{5.6}$$

If the orbital dependent functional $E^{\mathrm{xc}}[\phi_i[n]]$ is chosen to be the Hartree-Fock exchange functional, then the procedure just described leads to an orbital dependent exchange potential called "exact exchange", or EXX [82, 83]. In effect, in exact exchange a local exchange-correlation potential is fitted to the Hartree-Fock exchange. Interestingly, this leads to the correct asymptotic

behavior of the XC potential, because correlation is a short range phenomenon and the the long range potential is therefore solely determined by the exchange interaction. In 1992 Krieger, Li and Iafrate (KLI) [84] presented a, computationally less demanding, approximation to the EXX potentials, resulting in a orbital-dependent potential of the form

$$v_{\mathrm{KLI}}^{\mathrm{xc}} = v_{\mathrm{LSDA}}^{\mathrm{xc}} + \sum_{i=1}^{N} \frac{|\phi_i(r)|^2}{n(r)} v_i(r), \tag{5.7}$$

with orbital dependent potentials $v_i(r)$. The KLI potential has the correct asymptotics $-1/r$ and displays the integer discontinuity by construction. The orbital dependent potentials have no corresponding XC functional and therefore an energy expression is not available when using them.

The improved potentials presented so far all try to incorporate Hartree-Fock exchange to profit from its self-interaction correction. An investigation of both, methods that mix in HF exchange and localized Hartree-Fock methods can be found in a recent paper [85].

Based on the DD Casida *et. al* [86, 87] and Tozer and Handy [67] propose asymptotic corrections to XC potentials by adding a constant, which are derived from standard (semi-)local XC functionals. The resulting potentials go as $-(1/r) + I + \epsilon^{\mathrm{HOMO}}$ as r goes to infinity, where ϵ^{HOMO} is the HOMO eigenvalue obtained using the standard XC potential.

Baerends and coworkers proposed another line of XC potentials. Their ansatz was to model a potential that has the correct asymptotic $-1/r$ behavior and vanished at infinity. The first of these, the LB94 potential [71] does show the correct asymptotics but is somewhat less accurate than standard potentials near the nucleus. The next one, the GLB potential [88, 89], provides a better representation in the inner region but, while it does go to $-(1/r)$ asymptotically, it does so too slowly. Finally the statistical average of different orbital model potentials (SAOP) [90, 91, 45] was proposed, which interpolates between the GLB in the inner and a modified LB94 (LB-α) in the outer regions. As the name implies, the SAOP is orbital dependent, somewhat resembling the KLI potential (5.7).

In the present work, an efficient way to apply an improved XC potential to a TD-DFRT calculation is shown. We choose to implement an orbital dependent potential because these remain within the pure DFT formalism and because, upon investigating the effects of approximations in TD-DFRT, Petersilka, Gross and Burke [37] find that "the construction of approximate

exchange-correlation potentials based on orbital functions would be the method of choice for the future". In particular, we implement the SAOP potential, since it shows promising results in ground-state [90, 91, 45] and in response [45, 92] calculations and is *ab initio* in the sense that it is not fitted to a set of molecules. Of course the efficient procedure, described in the next section 5.2, can be applied to other potentials as well.

It should be noted, that the excitation energies are not the only response properties that are sometimes problematic when using the standard LDA/GGA functionals. Investigations of other response properties, like polarizabilities, hyperpolarizabilities, or Cauchy coefficients and find a similar picture as for the excitation energies [93, 45, 92]. These properties are also improved when using an accurate XC potential [45].

5.1.1 SAOP

We present only the final formulation of the SAOP potential as found in [45], leaving out the slightly different, older versions from [90, 91]. The SAOP is given by

$$v^{\mathrm{xc}}_{\mathrm{SAOP},\sigma}(r) = \sum_{i=1}^{N_\sigma} v^{\mathrm{xc}}_{\mathrm{mod},i\sigma}(r) \frac{|\phi_{i\sigma}(r)|^2}{n_\sigma(r)}, \tag{5.8}$$

where the $\phi_{i\sigma}(r)$ are the Kohn-Sham orbitals and the model potentials $v^{\mathrm{xc}}_{\mathrm{mod},i\sigma}(r)$ are obtained from an exponential interpolation between $v^{\mathrm{xc}}_{\mathrm{LB}\alpha,\sigma}(r)$ and $v^{\mathrm{xc}}_{\mathrm{GLB},\sigma}(r)$

$$v^{\mathrm{xc}}_{\mathrm{mod},i\sigma}(r) = e^{-2(\epsilon_{N\sigma}-\epsilon_{i\sigma})^2} v^{\mathrm{xc}}_{\mathrm{LB}\alpha,\sigma}(r) + (1 - e^{-2(\epsilon_{N\sigma}-\epsilon_{i\sigma})^2}) v^{\mathrm{xc}}_{\mathrm{GLB},\sigma}(r). \tag{5.9}$$

The LBα potential is a slightly modified LB94 potential, which was inspired by Becke's exchange functional [30]

$$v^{\mathrm{xc}}_{\mathrm{LB}\alpha,\sigma}(\alpha,\beta;r) = \alpha v^{\mathrm{x}}_{\mathrm{LDA},\sigma}(r) + v^{\mathrm{c}}_{\mathrm{LDA},\sigma}(r) - \frac{\beta x^2_\sigma(r) n^{1/3}_\sigma(r)}{1 + 3\beta x_\sigma(r) \ln\{x_\sigma(r) + [x^2_\sigma(r)+1]^{1/2}\}}. \tag{5.10}$$

Here $x_\sigma(r) = |\nabla n_\sigma(r)|/n^{-4/3}_\sigma(r)$ is the dimensionless gradient of the density and $v^{\mathrm{x}}_{\mathrm{LDA},\sigma}(r)$ and $v^{\mathrm{c}}_{\mathrm{LDA},\sigma}(r)$ are the LDA exchange and correlation potentials [16] respectively. In the CP2K implementation, the Perdew-Zunger [26] parameterization of the correlation potential is used. The constants α and β are fixed to $\alpha = 1.19$ and $\beta = 0.01$.

The GLB potential is another approximation of the exact XC potential with correct asymptotics. In addition the GLB also models the shell structure of the XC potential close to the nucleus. It consists of a hole part, which is just two times the exchange energy density of Becke [30] and two times the correlation energy density of Perdew and Wang [28], and a response potential, which resembles the response part of the KLI potential

$$v^{\mathrm{xc}}_{\mathrm{GLB},\sigma}(r) = 2\epsilon^{\mathrm{xc}}_{\mathrm{B},\sigma}(r) + 2\epsilon^{\mathrm{xc}}_{\mathrm{PW},\sigma}(r) + K_\sigma \sum_{i=1}^{N_\sigma} \sqrt{\epsilon_{N_\sigma} - \epsilon_{i\sigma}} \frac{|\phi_{i\sigma}(r)|^2}{n_\sigma(r)}. \tag{5.11}$$

where K_σ is fixed to 0.42. In CP2K the Perdew-Zunger energy density is used instead of the Perdew-Wang one.

Note that, even though it depends explicitly on the Kohn-Sham orbitals, the SAOP potential is still a functional of the density, in the sense of the Hohenberg-Kohn theorem. Therefore the use of the SAOP potential is a density functional method, because all the orbitals see the same potential, contrary to Hartree-Fock theory, where each orbital experiences a different interaction.

5.2 Two-step procedure to improve the excitation energies

Following what has been said in the previous section 5.1, we concentrate on the improvement of the orbital eigenvalues (or the Kohn-Sham matrix in the CP2K implementation) by using an accurate XC potential and do not modify the XC kernel.

But besides that an energy functional, and thus the total energy of the ground-state and excited states, is not available, the accurate XC potentials have another problem: They are computationally quite expensive and bring the scaling, of the construction of the Kohn-Sham matrix, from linear to quadratic. This is because, in a system with N electrons, N (or $N/2$ in a spin-restricted system) orbital densities have to be constructed on a grid (as explained in section 3.2), each of which scales linearly with the system size. Obviously, there's no way around this quadratic scaling, but we can try to keep the pre-factor as small as possible. In the Kohn-Sham scheme, the orbitals are optimized iteratively, using anywhere from a few to tens or even hundreds of iteration steps, depending on the algorithm used to find the orbitals. Each of these iteration steps requires the calculation of the Kohn-Sham matrix, which using an orbital dependent XC potential, scales quadratically. If it is possible to reduce the number of times the

orbital dependent XC potential has to be calculated, the pre-factor can be made smaller. In particular, for a large system, if the orbital dependent XC potential is calculated only once, the pre-factor is reduced by a factor given by the number of iteration steps needed.

The standard GGA XC functionals produce high quality results for ground-state properties. Therefore it is assumed, that the occupied Kohn-Sham orbitals, obtained using GGA functionals, are close approximations to the "true" Kohn-Sham orbitals, which are the orbitals resulting from the exact XC potential. This would mean that accurate XC potentials mainly improve the orbital eigenvalues. We exploit this in the two-step procedure by doing the TD-DFRT calculation in the following two steps:

1. A ground-state calculation is done using a standard XC functional.
2. The Kohn-Sham matrix is recalculated, but not diagonalized, using an accurate XC potential and a TD-DFRT calculation is done.

In this scheme, the orbital-dependent XC potential needs to be calculated only once instead of at every iteration step, greatly reducing the pre-factor compared to a self-consistent application of the orbital-dependent XC potential. In addition, the total energy of the ground-state and the excited states can be determined using the two-step procedure, since a potential with a corresponding functional is employed in the ground-state calculation.

The two-step procedure can be expected to increase the quality of the calculated Rydberg excitation energies at a relatively small computational cost, but it also has the disadvantage, that the Kohn-Sham orbitals are no longer the eigenvectors of the Kohn-Sham matrix. This complicates the assignment of the symmetry of the excitations.

5.2.1 Implementation in CP2K

The first step, of the two-step procedure, is just an ordinary ground-state calculation and nothing in the code has to be modified for this.

The SAOP potential is not yet part of the XC functional collection of CP2K. This means that it is not possible to just call the subroutine responsible for the construction of the Kohn-Sham matrix with the SAOP potential as argument to get the desired matrix for the two-step

procedure. Instead, that subroutine is called requesting no XC functional at all, resulting in a Kohn-Sham matrix that has no contribution from the XC potential. Then the SAOP XC potential is added separately onto this Kohn-Sham matrix. During these subroutine calls the electronic ground-state density and the Kohn-Sham orbitals remain unchanged. Once the Kohn-Sham matrix using the SAOP potential is obtained, the TD-DFRT routines are called and the excitation energy calculation proceeds as in the standard case.

The subroutine calculating the SAOP potential matrix elements uses the real-space grid representation of the electronic density $n_\sigma^{(0)}(r)$ and the orbital densities $|\phi_{i\sigma}(r)|^2$. To this end, the orbital density matrices $\mathbf{P}_\sigma^i$ are constructed

$$P^i_{\mu\nu\sigma} = c^{(0)}_{\mu i\sigma} c^{(0)}_{\nu i\sigma}. \tag{5.12}$$

These matrices are then passed to the subroutine that calculates the values of the density on the real-space grid. After computing the SAOP potential on the grid, it can be integrated onto the Kohn-Sham matrix using the integration routine from the standard calculation.

The two-step procedure is applicable to any computational method, be it plane waves with pseudopotentials, finite difference schemes or the GAPW method. However, for the GAPW method and an orbital-dependent potential we have to partition the orbital densities according to the GAPW scheme and then evaluate

$$\sum_{i=1}^{N_\sigma} v_i^{\mathrm{xc}}[n](r)\frac{|\phi_i(r)|^2}{n(r)} = \sum_{i=1}^{N_\sigma} v_i^{\mathrm{xc}}[\tilde{n} + \sum_A n_A - \sum_A \tilde{n}_A](r)\frac{|\tilde{\phi}_i(r)|^2 + \sum_B |\phi_{i,B}(r)|^2 - \sum_B |\tilde{\phi}_{i,B}(r)|^2}{\tilde{n}(r) + \sum_C n_C(r) - \sum_C \tilde{n}_C(r)}. \tag{5.13}$$

This means that there could be cross terms between hard and soft density parts. But again the locality of the involved XC potentials makes sure that this is not the case. The same reasoning, that leads to the separation of the hard and soft terms in the kernel calculation (see appendix B), leads to the separation of the hard and soft terms for the orbital-dependent potentials

$$\sum_{i=1}^{N_\sigma} v_i^{\mathrm{xc}}[n](r)\frac{|\phi_i(r)|^2}{n(r)} = \sum_{i=1}^{N_\sigma}\left[v_i^{\mathrm{xc}}[\tilde{n}](r)\frac{|\tilde{\phi}_i(r)|^2}{\tilde{n}(r)} + \sum_A v_i^{\mathrm{xc}}[n_A](r)\frac{|\phi_{i,A}(r)|^2}{n_A(r)} - \sum_A v_i^{\mathrm{xc}}[\tilde{n}_A](r)\frac{|\tilde{\phi}_{i,A}(r)|^2}{\tilde{n}_A(r)}\right]. \tag{5.14}$$

5.3 Test calculations

Test calculations on the same molecules as the ones used in chapter 3 and 4 were done using the two-step procedure. We show results for the GPW implementation in tables 5.1 and 5.2, where the values calculated using the PBE functional are in the column labeled "GPW/PBE" and the two-step corrected values are in the column labeled "GPW/2S.-SAOP". We use the same calculation parameters as in the test calculations in chapter 3. In addition, for the molecules with a spin-restricted ground-state, we present excitation energies obtained using a self-consistent application of the SAOP potential. These are taken from [45] and [46] and calculated using the ADF program. Since these are taken from the same source as the ADF LDA values presented in chapter 3, the same reservations as in that chapter apply.

We note, that using the two-step procedure with the SAOP potential, it is not possible to assign definite calculated excitation energies for the two highest singlet and triplet excitation energies of formaldehyde and the highest singlet excitation energy of acetone. The symmetry of the excitations is given by the product of the symmetry of the involved orbitals. But in the two-step procedure the Kohn-Sham orbitals are not the eigenvectors of the Kohn-Sham matrix. Therefore, in the two-step procedure, excitations can be linear combinations of orbital transitions which have different symmetries according to the XC functional used in the first step. This problem is most severe for excitations that are linear combinations of a large number of orbital transitions with small coefficients.

The large deviations of the excitation energies of the ADF values of water and experiment are due to the small basis set employed in the ADF calculation. This has the same effect as in the calculation using LDA, reported in chapter 3. This shows that a sufficiently complete basis set is also necessary when using accurate XC potentials. In the subsequent analysis the ADF water values and the ambiguous two-step values are excluded.

Table 5.2 gives the AAD of the used methods and functionals with experiment. We find a degradation in the quality, of the predicted valence excitation energies, from an AAD of 0.184 eV to 0.390 eV, when using the two-step procedure. Recall, that the valence excitations are dominated by the XC potential near the atomic cores. Therefore we conclude, that the SAOP potential, determined using the Kohn-Sham orbitals corresponding to the PBE functional, differs

Molecule	State	GPW/PBE	GPW/2S.-SAOP	ADF	Exp.
N_2	$V^1\ \Pi_g$	9.295	9.366	9.31	9.31
	$V^1\ \Sigma_u^-$	9.688	9.647	9.66	9.92
	$V^1\ \Delta_u$	10.197	10.162	10.21	10.27
	$V^3\ \Sigma_u^+$	7.704	7.748	7.89	7.75
	$V^3\ \Pi_g$	7.945	7.906	7.81	8.04
	$V^3\ \Delta_u$	8.836	8.794	8.82	8.88
CO	$V^1\ \Pi$	8.535	8.444	8.56	8.51
	$V^1\ \Sigma^-$	9.861	10.376	10.03	9.88
	$V^1\ \Delta$	10.276	10.802	10.46	10.23
	$V^3\ \Pi$	6.173	5.848	6.28	6.32
	$V^3\ \Sigma^+$	8.413	8.906	8.64	8.51
	$V^3\ \Delta$	9.160	9.661	9.37	9.36
	$V^3\ \Sigma^-$	9.861	10.376	10.03	9.88
H_2O	$R^1\ B_1$	6.378	8.335	10.35	7.4
	$R^1\ A_2$	7.669	9.453	12.23	9.1
	$R^1\ A_1$	8.511	10.285	12.41	9.7
	$R^1\ B_1$	8.952	10.961	17.14	10.0
	$R^1\ A_1$	9.344	11.397	18.06	10.17
	$R^3\ B_1$	6.124	7.845		7.2
C_2H_4	$R^1\ B_{3u}$	6.427	7.104	7.29	7.11
	$V^1\ B_{1u}$	7.683	8.013	7.62	7.60
	$R^1\ B_{1g}$	6.972	7.644	8.00	7.80
	$R^1\ B_{2g}$	6.940	7.670	7.94	8.01
	$R^1\ A_g$	7.776	9.028	8.91	8.29
	$R^1\ B_{3u}$	8.147	8.764	9.03	8.62
	$V^3\ B_{1u}$	4.719	4.667	4.64	4.36
	$R^3\ B_{3u}$	6.378	6.990	7.18	6.98
	$R^3\ B_{1g}$	6.958	7.223	7.91	7.79
	$R^3\ B_{2g}$	6.892	7.552	7.81	7.79
	$R^3\ A_g$	7.520	8.705	8.70	8.15
CH_2O	$V^1\ A_2$	3.777	4.450	4.24	4.07
	$R^1\ B_2$	5.757	7.794	7.14	7.11
	$R^1\ B_2$	6.752	9.010	8.21	7.97
	$R^1\ A_1$	6.519	8.569	8.26	8.14
	$R^1\ A_2$	7.112	$\leq$10.496		8.37
	$R^1\ B_2$	8.036	$\leq$10.584		8.88
	$V^3\ A_2$	3.150	3.807	3.64	3.50
	$V^3\ A_1$	6.045	6.316	6.33	5.86
	$R^3\ B_2$	5.703	7.527	6.92	6.83
	$R^3\ B_2$	6.700	$\geq$ 8.123	8.08	7.79
	$R^3\ A_1$	6.497	$\geq$ 8.123	8.15	7.91
$CO(CH_3)_2$	$V^1\ A_2$	4.239	4.901	4.58	4.35
	$R^1\ B_2$	4.956	6.953	6.16	6.34
	$R^1\ A_2$	5.951	8.390	7.56	7.36
	$R^1\ A_1$	5.779	8.154	7.38	7.40
	$R^1\ B_2$	6.101	$\geq$8.607	7.90	7.45
	$V^3\ A_2$	3.706	4.354		4.16
	$V^3\ A_1$	5.691	6.874		5.88

Table 5.1: Calculated and experimental excitation energies, in electronvolts, of test molecules. See chapter 3 for more information on geometries and experimental values.

Molecule	State	GPW/PBE	GPW/2S.-SAOP	Exp.
BeH	V Π	2.644	3.290	2.48
	R Π	5.908	6.237	6.32
BeF	V Π	4.242	4.650	4.14
	R Σ^+	5.602	6.500	6.16
	R Σ^+	6.484	7.747	6.27
CN	V Π	2.089	2.220	1.32
	V Σ^+	3.678	3.697	3.22
CH_3	R A_1'	4.900	6.437	5.73
	R A_2''	6.266	8.430	7.44

Table 5.2: Calculated and experimental singlet excitation energies, in electronvolts, of test molecules. See chapter 3 for more information on geometries and experimental values.

	GPW/PBE - Exp.	GPW/2S.-SAOP - Exp.	ADF - Exp.
V	0.184 $\pm$ 0.180	0.390 $\pm$ 0.258	0.148 $\pm$ 0.118
R	1.03 $\pm$ 0.361	0.604 $\pm$ 0.379	0.223 $\pm$ 0.174

Table 5.3: Average absolute deviations of the methods and experiment and standard deviation thereof in electronvolts

from the PBE XC potential in this region. Indeed, it is found that the effect of the accurate XC potentials is not only important in the asymptotic region, but also in the inner regions [92]. The AAD of the ADF values cannot be directly compared to the AAD obtained with the two-step procedure, since we have fewer results with the ADF program. In particular, we do not have results for the molecules with a spin-unrestricted ground-state wavefunction, which, on the average, have a larger deviation than the spin-restricted molecules when using the GPW or GAPW methods. Nevertheless, we can interpret the AADs of the values obtained with ADF as an indicator of the accuracy, that can be achieved, if the SAOP potential is applied self-consistently. The low AAD of 0.148 eV for valence excitations suggests, that, if the orbitals are allowed to relax, then the quality of the valence excitation energy should be equal to the ones obtained with a standard GGA functional.

For the Rydberg excitations however, we find, that using the two-step procedure leads to a significant improvement of the excitation energies from an AAD of 1.03 eV, with the PBE potential, to 0.604 eV. Looking at the individual values, it is noted, that the two-step procedure often over corrects the Rydberg excitation energies, so that the two-step values are higher than the experimental energies, while they are too low using the PBE potential. Again the AADs of the ADF values indicate, that a self-consistent application of the SAOP potential can achieve an even better performance for the Rydberg excitations.

In conclusion, we find that the two-step procedure is able to fulfill its intended role of improving the predicted Rydberg excitation energies. However it is conceivable, that better results are obtained if it is possible to find Kohn-Sham orbitals which approximate the self-consistent SAOP orbitals more closely. This could be achieved, for example, by applying the accurate XC potential semi-self-consistently by doing one or more iterations. It is also possible, that another GGA or LDA functional gives better approximates to the SAOP orbitals.

Chapter 6

Conclusions and outlook

In this work, we present computationally efficient implementations, of linear response TD-DFT for the calculation of excitation energies, in a computer program called CP2K [39]. The implementation in the GPW and pseudopotential framework is shown to yield reliable results, while retaining the favorable scaling behavior of the method. It does so, by using the localization of the atomic basis functions and the evaluation of the Hartree potential in reciprocal space using fast Fourier transform techniques. Test calculations using the PBE XC functional produce high quality valence and deficient Rydberg excitation energies in agreement with the literature.

The GAPW implementation uses two different types of functions to represent the electronic density. Thereby it is possible to do calculations including all electrons of a system while retaining the linear scaling behavior that the GPW method already provides. Test calculations show that TD-DFRT with the GAPW method gives the same reliable results as the GPW method implementation.

In addition we present the two-step procedure, which can improve the calculated Rydberg excitation energies while still providing the total energy of the ground-state and excited states. This is achieved by evaluating an accurate XC potential at the density of the ground-state obtained with a standard XC functional. The computational cost of this procedure scales quadratically with the system size, but compares favorably with other ways of improving the Rydberg excitation energies.

6.1 Outlook

We concentrated on small systems of atoms and molecules in the gas phase, where the ALDA gives good results, but the methods presented in this documents are also applicable to condensed matter. The electronic structure of a molecule in the liquid phase, where the bonding between the molecules arises from Van der Waals and electrostatic interactions, is to a large degree similar to the electronic structure in the gas phase. Therefore the presented methods can be expected to be useful in the liquid phase as well. In electronic band calculations of condensed matter, however, the non-local character of the XC kernel should be taken into account [94]. The performance of the presented methods in the liquid and the solid phase should be investigated.

The electronic excitations are not completely characterized by their excitation energy and symmetry. The oscillation strengths, which give the transition probabilities are of equal interest. The molecular TD-DFRT formalism [15] provides a way to calculate the oscillator strengths but this is not applicable to extended systems. Recently [77] a formulation in terms of the Berry phase polarization has been given that could be applied to the methods presented here.

The calculation of excitation energies is but one of the possible response properties that can be calculated. The implementation of polarizabilities, NMR chemical shifts and other response properties using the GPW and GAPW methods is under way. Also, it would be interesting to implement the calculation of excited state properties, like excited state forces and dipole moments, presented in [69], for example.

With the ongoing miniaturization in technology and, as consequence thereof, with increasing interest in photonic applications, the computational treatment of electronic excitations is gaining importance. Due its favorable scaling, TD-DFRT has the potential to become a very important computational tool in this growing field of science.

Appendix A

Functional derivatives and the linear response kernel

This appendix demonstrates how to calculate the XC part of the linear response kernel in the adiabatic and local approximation for a spin-restricted density. The most general, spin-unrestricted case, is simply stated at the end of the chapter. The formulas can be found, together with specific formulas for common GGA functionals, in [95].

The integral to be calculated is

$$\int \left.\frac{\delta^2 E^{\mathrm{xc}}[n,|\nabla n|]}{\delta n(r)\delta n(r')}\right|_{n^{(0)}(r)} n^{(1)}(r')dr' = \int \left.\frac{\delta v^{\mathrm{xc}}[n,|\nabla n|](r)}{\delta n(r')}\right|_{n^{(0)}(r)} n^{(1)}(r')dr' \tag{A.1}$$

where $E^{\mathrm{xc}}[n]$ is a local functional of the density n and its gradient $|\nabla n|$. For this calculation the XC potential has to be considered to depend only parametrically on r. With a local XC functional [1]

$$E^{\mathrm{xc}}[n] = \int e^{\mathrm{xc}}(n(r),|\nabla n|(r))dr \tag{A.2}$$

the XC potential becomes

$$v^{\mathrm{xc}}[n,|\nabla n|](r) = \frac{\partial e^{\mathrm{xc}}}{\partial n}(r) - \nabla \frac{\partial e^{\mathrm{xc}}}{\partial |\nabla n|}(r)\frac{\nabla n(r)}{|\nabla n(r)|} \tag{A.3}$$

[1] Note that this definition differs from the customary definition in the literature $E^{\mathrm{xc}}[n] = \int n(r) e^{\mathrm{xc}}(n(r),|\nabla n|(r))dr$. This definition, however, causes more terms to appear in the derivative because of the extra product and is notationally more cumbersome.

The functional derivative $\frac{\delta F}{\delta f}$ of a Functional $F[f]$ is defined as follows

$$\int \frac{\delta F}{\delta f(r)} u(r)\, dr = \frac{d}{d\varepsilon} F[f(r) + \varepsilon u(r)]\Big|_{\varepsilon=0}. \tag{A.4}$$

Applying this to the XC potential we find

$$\int \frac{\delta^2 E^{\mathrm{xc}}[n, |\nabla n|]}{\delta n(r)\delta n(r')}\Big|_{n^{(0)}(r)} n^{(1)}(r')dr' = \frac{d}{d\varepsilon}\, v^{\mathrm{xc}}[n + \varepsilon n^{(1)}, |\nabla n + \varepsilon \nabla n^{(1)}|]\Big|_{\varepsilon=0, n=n^{(0)}} = \frac{\partial}{\partial n} v^{\mathrm{xc}}[n, |\nabla n|] n^{(1)} + \frac{\partial}{\partial \nabla n} v^{\mathrm{xc}}[n, |\nabla n|] \nabla n^{(1)}. \tag{A.5}$$

Using $\partial/\partial \nabla n = \partial/\partial |\nabla n| \cdot (\nabla n/|\nabla n|)$ (A.5) results in

$$\int \frac{\delta^2 E^{\mathrm{xc}}[n, |\nabla n|]}{\delta n(r)\delta n(r')}\Big|_{n^{(0)}(r)} n^{(1)}(r')dr' = \left\{ \frac{\partial^2 e^{\mathrm{xc}}}{\partial n^2} n^{(1)} + \frac{\partial^2 e^{\mathrm{xc}}}{\partial n \partial |\nabla n|} \frac{\nabla n}{|\nabla n|} \nabla n^{(1)} - \nabla \left[\frac{\partial^2 e^{\mathrm{xc}}}{\partial n \partial |\nabla n|} \frac{\nabla n}{|\nabla n|} n^{(1)} \frac{\partial^2 e^{\mathrm{xc}}}{\partial |\nabla n|^2} \frac{\nabla n}{|\nabla n|} \frac{\nabla n}{|\nabla n|} \nabla n^{(1)} + \frac{\partial e^{\mathrm{xc}}}{\partial |\nabla n|} \left(\frac{\nabla n^{(1)}}{|\nabla n|} - \frac{\nabla n}{|\nabla n|^3} \nabla n \cdot \nabla n^{(1)} \right) \right] \right\} \Big|_{n=n^{(0)}} \tag{A.6}$$

A.1 Second derivative in the spin-unrestricted case

The following formula gives the $(\alpha, \alpha) + (\alpha, \beta)$ spin contribution, needed for spin-restricted singlets and the spin-unrestricted α-spin density. To get the $(\alpha, \alpha) - (\alpha, \beta)$ contribution, for the spin-restricted triplets, change the sign of the $n_\beta^{(1)}$ terms. To get the $(\alpha, \beta) + (\beta, \beta)$ contribution, needed in the spin-unrestricted β-spin density, interchange α and β in the $n_\alpha^{(1)}$ terms.

(A.7)

$$
\begin{aligned}
&\sum_{\tau=\alpha,\beta}\int dr\ \frac{\delta^2 E^{\mathrm{xc}}[n_\alpha,n_\beta,|\nabla n_\alpha|,|\nabla n_\beta|,|\nabla n|]}{\delta n_\alpha(r)\delta n_\tau(r)}\bigg|_{n=n^{(0)}} n_\tau^{(1)}(r)\\
&=\Bigg\{\frac{\partial^2 e^{\mathrm{xc}}}{\partial {n_\alpha}^2}n_\alpha^{(1)}+\frac{\partial^2 e^{\mathrm{xc}}}{\partial n_\alpha\partial n_\beta}n_\beta^{(1)}+\frac{\partial^2 e^{\mathrm{xc}}}{\partial n_\alpha\partial|\nabla n_\alpha|}\frac{\nabla n_\alpha\nabla n_\alpha^{(1)}}{|\nabla n_\tau|}+\frac{\partial^2 e^{\mathrm{xc}}}{\partial n_\alpha\partial|\nabla n_\beta|}\frac{\nabla n_\beta\nabla n_\beta^{(1)}}{|\nabla n_\beta|}+\\
&+\frac{\partial^2 e^{\mathrm{xc}}}{\partial n_\alpha\partial|\nabla n|}\frac{\nabla n_\beta\nabla n_\alpha^{(1)}+\nabla n_\alpha\nabla n_\beta^{(1)}}{|\nabla n|}-\nabla\Bigg[\frac{\nabla n_\alpha}{|\nabla n_\alpha|}\Bigg(\frac{\partial^2 e^{\mathrm{xc}}}{\partial n_\alpha\partial|\nabla n_\alpha|}n_\alpha^{(1)}+\frac{\partial^2 e^{\mathrm{xc}}}{\partial n_\beta\partial|\nabla n_\alpha|}n_\beta^{(1)}\\
&+\frac{\partial^2 e^{\mathrm{xc}}}{\partial|\nabla n_\alpha|\partial|\nabla n|}\frac{\nabla n_\beta\nabla n_\alpha^{(1)}+\nabla n_\alpha\nabla n_\beta^{(1)}}{|\nabla n|}+\frac{\partial^2 e^{\mathrm{xc}}}{\partial|\nabla n_\alpha|^2}\frac{\nabla n_\alpha\nabla n_\alpha^{(1)}}{|\nabla n_\alpha|}+\frac{\partial^2 e^{\mathrm{xc}}}{\partial|\nabla n_\alpha|\partial|\nabla n_\beta|}\frac{\nabla n_\beta\nabla n_\beta^{(1)}}{|\nabla n_\beta|}\\
&-\frac{\partial e^{\mathrm{xc}}}{\partial|\nabla n_\alpha|}\frac{\nabla n_\alpha\nabla n_\alpha^{(1)}}{|\nabla n_\alpha|^2}\Bigg)+\nabla n_\beta\Bigg(\frac{\partial^2 e^{\mathrm{xc}}}{\partial n_\alpha\partial|\nabla n|}\frac{n_\alpha^{(1)}}{|\nabla n|}+\frac{\partial^2 e^{\mathrm{xc}}}{\partial|\nabla n_\alpha|\partial|\nabla n|}\frac{\nabla n_\alpha\nabla n_\alpha^{(1)}}{|\nabla n||\nabla n_\alpha|}\\
&+\frac{\partial^2 e^{\mathrm{xc}}}{\partial n_\beta\partial|\nabla n|}\frac{n_\beta^{(1)}}{|\nabla n|}+\frac{\partial^2 e^{\mathrm{xc}}}{\partial|\nabla n_\beta|\partial|\nabla n|}\frac{\nabla n_\beta\nabla n_\beta^{(1)}}{|\nabla n||\nabla n_\beta|}+\frac{\partial^2 e^{\mathrm{xc}}}{\partial|\nabla n|^2}\frac{\nabla n_\beta\nabla n_\alpha^{(1)}+\nabla n_\alpha\nabla n_\beta^{(1)}}{|\nabla n|^2}\Bigg)\\
&+\frac{\partial e^{\mathrm{xc}}}{\partial|\nabla n_\alpha|}\frac{\nabla n_\alpha^{(1)}}{|\nabla n_\alpha|}+\frac{\partial e^{\mathrm{xc}}}{\partial|\nabla n|}\frac{\nabla n_\beta^{(1)}}{|\nabla n|}\Bigg]\Bigg\}\Bigg|_{n=n^{(0)}}
\end{aligned}
$$

Appendix B

Calculation of the second derivatives of the XC functional in the GAPW method

In this section, it is demonstrated, how the evaluation of the XC term of the linear response potential

$$\int dr \left.\frac{\delta^2 E^{\mathrm{xc}}[n]}{\delta n_\sigma(r)\delta n_\tau(r)}\right|_{n=\tilde{n}^{(0)}+\sum_A n_A^{(0)}-\sum_A \tilde{n}_A^{(0)}} \{\tilde{n}^{(1)}(r)+\sum_B n^{(1)}(r)-\sum_B \tilde{n}_B^{(1)}(r)\} \tag{B.1}$$

results in terms to be evaluated on the corresponding density parts of the ground state $n^{(0)}$ and the linear response density $n^{(1)}$.

To make the notation less cumbersome, the abbreviation $f(x)$ for the second functional derivative of the XC functional is introduced

$$f(x)y \equiv \int dr \left.\frac{\delta^2 E^{\mathrm{xc}}[n]}{\delta n_\sigma(r)\delta n_\tau(r)}\right|_{n=x} y(r). \tag{B.2}$$

Now (B.1) can be rewritten as

$$f(\tilde{n}^{(0)}+\sum_A n_A^{(0)}-\sum_A \tilde{n}_A^{(0)})\{\tilde{n}^{(1)}(r)+\sum_B n^{(1)}(r)-\sum_B \tilde{n}_B^{(1)}(r)\} \tag{B.3}$$

and because the XC functional is local in space this is equal to

$$\left[f(\tilde{n}^{(0)}) + \sum_A f(n_A^{(0)}) - \sum_A f(\tilde{n}_A^{(0)})\right]\{\tilde{n}^{(1)}(r) + \sum_B n^{(1)}(r) - \sum_B \tilde{n}_B^{(1)}(r)\}. \tag{B.4}$$

Now every term in the rectangular braces is evaluated separately in the interstitial region I and in the atomic region C. For the first term

$$f(\tilde{n}^{(0)})\{\tilde{n}^{(1)}(r) + \sum_B n^{(1)}(r) - \sum_B \tilde{n}_B^{(1)}(r)\} \tag{B.5}$$

we find

$$f(\tilde{n}^{(0)})\tilde{n}^{(1)} \quad \text{for } r \in I \tag{B.6}$$

because all the atom centered linear response densities cancel in I. And

$$f(\tilde{n}^{(0)})n_C^{(1)} \quad \text{in } r \in C \tag{B.7}$$

because the linear response densities centered on the atoms other than C cancel and the overall soft response density cancels with the soft response density centered on C. Using similar arguments the other two terms can be evaluated, which yields

$$\sum_A f(n_A^{(0)})\{\tilde{n}^{(1)}(r) + \sum_B n^{(1)}(r) - \sum_B \tilde{n}_B^{(1)}(r)\} = \begin{cases} \sum_A f(n_A^{(0)})\tilde{n}^{(1)} & r \in I, \\ \sum_A f(n_A^{(0)})n_C^{(1)} & r \in C \end{cases} \tag{B.8}$$

and

$$\sum_A f(\tilde{n}_A^{(0)})\{\tilde{n}^{(1)}(r) + \sum_B n^{(1)}(r) - \sum_B \tilde{n}_B^{(1)}(r)\} = \begin{cases} \sum_A f(\tilde{n}_A^{(0)})\tilde{n}^{(1)} & r \in I, \\ \sum_A f(\tilde{n}_A^{(0)})n_C^{(1)} & r \in C. \end{cases} \tag{B.9}$$

Taking the sum of the interstitial terms, it is found that

$$f(\tilde{n}^{(0)})\tilde{n}^{(1)} + \sum_A f(n_A^{(0)})\tilde{n}^{(1)} + \sum_A f(\tilde{n}_A^{(0)})\tilde{n}^{(1)} = f(\tilde{n}^{(0)})\tilde{n}^{(1)}, \quad \text{for } r \in I \tag{B.10}$$

because $n_A^{(1)} = \tilde{n}_A^{(1)}$ there. And in the atom centered region C, it is found that

$$f(\tilde{n}^{(0)})n_C^{(1)} + \sum_A f(n_A^{(0)})n_C^{(1)} + \sum_A f(\tilde{n}_A^{(0)})n_C^{(1)} = f(n_C^{(0)})n_C^{(1)}, \quad \text{for } r \in C \tag{B.11}$$

because the ground state densities centered on the atoms other than C cancel and the overall soft ground state density cancels with the soft response density centered on C and the XC functional is local in space. Finally, using the same line of arguments as already used in this appendix, we may add

$$\sum_A f(n_A^{(0)})n_A^{(1)} - \sum_A f(\tilde{n}_A^{(0)})\tilde{n}_A^{(1)} = 0 \quad \text{for } r \in I$$

to $f(\tilde{n}^{(0)})\tilde{n}^{(1)}$ and

$$f(\tilde{n}^{(0)})\tilde{n}^{(1)} - f(\tilde{n}_C^{(0)})\tilde{n}_C^{(1)} + \sum_{A\neq C} f(n_A^{(0)})n_A^{(1)} - \sum_{A\neq C} f(\tilde{n}_A^{(0)})\tilde{n}_A^{(1)} = 0 \quad \text{for } r \in C$$

to $f(n_C^{(0)})n_C^{(1)}$ to get the desired result

$$\text{(B.12)} \quad f(\tilde{n}^{(0)} + \sum_A n_A^{(0)} - \sum_A \tilde{n}_A^{(0)})\{\tilde{n}^{(1)}(r) + \sum_B n^{(1)}(r) - \sum_B \tilde{n}_B^{(1)}(r)\} = f(\tilde{n}^{(0)})\tilde{n}^{(1)} + \sum_A f(n_A^{(0)})n_A^{(1)} - \sum_A f(\tilde{n}_A^{(0)})\tilde{n}_A^{(1)}.$$

Appendix C

Definitions

Rydberg orbital From [96]: "For an atom, an orbital with principal quantum number greater than that of any occupied orbital of the ground state. For a molecular entity, a molecular orbital which correlates with a Rydberg atomic orbital in an atomic fragment produced by dissociation. Typically, the extension of the Rydberg orbital is large compared to the size of the atom or molecular entity."

Rydberg transition From [96]: "An electronic transition described approximately as promotion of an electron from a 'bonding' orbital to a Rydberg orbital. Spectral bands corresponding to Rydberg transitions approximately fit the Rydberg formula:

$$\sigma = I - R/(n - \Delta)^2$$

where σ is the wavenumber, I the ionization potential of the atom or molecular entity, n a principal quantum number, R the Rydberg constant, and Δ the quantum defect which differentiates between s,p,d, etc., orbitals."

Bibliography

[1] Attila Szabo and Neil S. Ostlund. *Modern Quantum Chemistry.* McGraw-Hill Publishing Company, 1989.

[2] Frank Jensen. *Introduction to Computational Chemistry.* John Wiley & Sons, 1999.

[3] L. H. Thomas. The calculation of atomic fields. *Proc. Cambridge Phil. Roy. Soc.*, 23:542 – 548, 1927.

[4] E. Fermi. Un metodo statistico per la determinazione di alcune priorieta dell'atome. *Accad. Naz. Lincei*, 6:602–607, 1927.

[5] P. A. M. Dirac. Note on exchange phenomena in the Thomas-Fermi atom. *Proc. Cambridge Phil. Roy. Soc.*, 26:376 – 385, 1930.

[6] P. Hohenberg and Kohn W. Inhomogeneous Electron Gas. *Physical Review*, 136(3B):B864 – B871, 1964.

[7] W. Kohn and L. J. Sham. Self-Consistent Equations Including Exchange and Correlation Effects. *Physical Review*, 140(4A):A1133 – A1138, 1965.

[8] A. Zangwill and Soven Paul. Density-functional approach to local-field effects in finite field systems: Photoabsorption in the rare gas. *Physical Review A*, 21(5):1561 – 1572, 1980.

[9] B. M. Deb and S. K. Gosh. Schrödinger fluid dynamics of many-electron systems in a time-dependent density-functional framework. *Journal of Chemical Physics*, 77(1):324 – 348, 1982.

[10] L. J. Bartolotti. Time-dependent extension of the Hohenberg-Kohn-Levy energy-density functional. *Physical Review A*, 24(4):1661 – 1667, 1981.

[11] Libero J. Bartolotti. Time-dependent Kohn-Sham density-functional theory. *Physical Review A*, 26(4):2243 – 2244, 1982.

[12] Libero J. Bartolotti. Variation-perturbation theory within a time-dependent Kohn-Sham formalism: An application to the determination of multipole polarizabilities, spectral sums, and dispersion coefficients. *Journal of Chemical Physics*, 80(11):5687 – 5695, 1984.

[13] Libero J. Bartolotti. Velocity form of the Kohn-Sham frequency-dependent polarizability equations. *Physical Review A*, 36(9):4492 – 4493, 1987.

[14] Erich Runge and E. K. U. Gross. Density-functional Theory for Time-Dependent Systems. *Physical Review Letters*, 52(12):997, 1984.

[15] M. E. Casida. In D. P. Chong, editor, *Recent Advances in Computational Chemistry*, volume 1, page 155. World Scientific, Singapore, 1995.

[16] Robert G. Parr and Weitao Yang. *Density-Functional Theory of Atoms and Molecules*. Oxford University Press, New York, 1989.

[17] R. M. Martin. *Electronic Structure: basic theory and practical methods*. Cambridge University Press, 2004.

[18] E. K. U. Gross, J. Dobson, and M. Petersilka. Density functional theory of time-independent phenomena. In R. F. Nalewajski, editor, *Density Functional Theory*, Topics in Current Chemistry. Springer, 1996.

[19] E. K. U. Gross and W. Kohn. Time-dependent density-functional theory. *Advances in Quantum Chemistry*, 21:255 – 291, 1990.

[20] Robert van Leeuwen. Causality and Symmetry in Time-Dependent Density-Functional Theory. *Physical Review Letters*, 80(6):1280 – 1283, 1998.

[21] A. L. Fetter and J. D. Walecka. *Quantum Theory of Many-Particle Systems*. McGraw-Hill, New York, 1971.

[22] So Hirata and Martin Head-Gordon. Time-dependent density functional theory within the Tamm-Dancoff approximation. *Chem. Phys. Lett.*, 314:291–299, 1999.

[23] H. Appel, E. K. U. Gross, and K. Burke. Excitations in Time-Dependent Density-Functional Theory. *Physical Review Letters*, 90(4):43005, 2003.

[24] D. M. Ceperley and B. J. Alder. Ground State of the Electron Gas by a Stochastic Method. *Physical Review Letters*, 45(7):566 – 569, 1980.

[25] G. Ortiz and P. Ballone. Correlation energy, structure factor, radial distribution function, and momentum distribution of the spin-polarized uniform electron gas. *Physical Review B*, 50(3):1391 – 1405, 1994.

[26] J. P. Perdew and Alex Zunger. Self-interaction correction to density-functional approximations for many-electron systems. *Physical Review B*, 23(10):5048 – 5079, 1981.

[27] S. Vosko, L. Wilk, and M. Nusair. Accurate spin-dependent electron liquid correlation energies for local spin density calculations: a critical analysis. *Canadian Journal of Physics*, 58:1200, 1983.

[28] John P. Perdew and Yue Wang. Accurate and simple analytic representation of the electron-gas correlation energy. *Physical Review B*, 45(23):13244 – 13249, 1992.

[29] S. Goedecker, M. Teter, and J. Hutter. Separable dual-space Gaussian pseudopotentials. *Physical Review B*, 54:1703 – 1710, 1996.

[30] A. D. Becke. Density-functional exchange-energy approximation with correct asymptotic behavior. *Physical Review A*, 39(6):3098 – 3100, 1988.

[31] John P. Perdew, Kieron Burke, and Matthias Ernzerhof. Generalized gradient approximation made simple. *Physical Review Letters*, 77(18):3865 – 3868, 1996.

[32] Chengteh Lee, Weitao Yang, and Robert G. Parr. Development of the Colle-Salvetti correlation-energy formula into a functional of the electron density. *Physical Review B*, 37(2):785 – 789, 1988.

[33] E. K. U. Gross and Walter Kohn. Local Density-Functional Theory of Frequency-Dependent Linear Response. *Physical Review Letters*, 55(26):2850 – 2852, 1985.

[34] S. J. A. van Gisbergen, F. Kootstra, P. R. T. Schipper, O. V. Gritsenko, J. G. Snijders, and E. J. Baerends. Density-functional-theory response-property calculations with accurate exchange-correlation potentials. *Physical Review A*, 57(4):2556 – 2571, April 1998.

[35] I. V. Tokatly and O. Pankratov. Many-Body Diagrammatic Expansion in a Kohn-Sham Basis: Implications for Time-Dependent Density Functional Theory of Excited States. *Physical Review Letters*, 86(10):2078 – 2081, 2001.

[36] S. Obara and K. Saika. Efficient recursive computation of molecular integrals over Cartesian Gaussian functions. *Journal of Chemical Physics*, 84(7):3963 – 3974, 1985.

[37] M. Petersilka, E. K. U. Gross, and Kieron Burke. Excitation Energies from Time-Dependent Density Functional Theory Using Exact and Approximate Potentials. *International Journal of Quantum Chemistry*, 80:534 – 554, 2000.

[38] Rüdiger Bauernschmitt, Marco Häser, Oliver Treutler, and Reinhart Ahlrichs. Calculation of excitation energies within time-dependent density functional theory using auxiliary basis set expansions. *Chem. Phys. Lett.*, 264:573, 1997.

[39] The CP2K developers group. http://cp2k.berlios.de, 2005.

[40] Joost VandeVondele, Matthias Krack, Fawzi Mohamed, Parrinello Michele, Thomas Chassaing, and Jürg Hutter. Quickstep: fast and accurate density functional calculations using a mixed Gaussian and plane waves approach. *Computer Physics Communications*, 167:103 – 128, 2005.

[41] Jürg Hutter. Excited state nuclear forces from the Tamm-Dancoff approximation to time-dependent density functional theory within the plane wave basis set framework. *Journal of Chemical Physics*, 118(9):3928, 2003.

[42] James W. Demmel. *Applied Numerical Linear Algebra*. SIAM, 1997.

[43] Ernest R. Davidson. The Iterative Calculation of a Few of the Lowest Eigenvalues and Corresponding Eigenvectors of Large Real-Symmetric Matrices. *Journal of Computational Physics*, 17:87 – 94, 1975.

[44] O. Treutler and R. Ahlrichs. TURBOMOLE V. 5.6. www.turbomole.com.

[45] P. R. T. Schipper, O. V. Gritsenko, S. J. A. Grisbergen, and E. J. Baerends. Molecular calculations of excitation energies and (hyper)polarizabilities with a statistical average of orbital model exchange-correlation potentials. *Journal of Chemical Physics*, 112(3):1344 – 1352, 2000.

[46] Johannes Neugebauer. Private communication, May 2005.

[47] The CPMD consortium. http://www.cpmd.org, 2004.

[48] David Maurice and Martin Head-Gordon. Configuration Interaction with Single Substitutions for Excited States of Open-Shell Molecules. *International Journal of Quantum Chemistry*, 29:361 – 370, 1995.

[49] Jens Oddershede, Norbert E. Grüner, and Gerd H.F Diercksen. Comparison between equation of motion and polarization propagator calculations. *Chemical Physics*, 97:303 –310, 1985.

[50] Egon s. Nielsen, Poul Jørgensen, and Jens Oddershede. Transition moments and dynamic polarizabilities in a second order polarization propagator approach. *Journal of Chemical Physics*, 73(12):6238 – 6246, 1980.

[51] Kenneth B. Wiberg, Christopher M. Hadad, James B. Foresman, and William A. Chupka. Electronically Excited States of Ethylene. *Journal of Physical Chemistry*, 96(26):10756 – 10768, 1992.

[52] Christopher M. Hadad, James B. Foresman, and Kenneth B. Wiberg. Excited States of Carbonyl Compounds. 1. Formaldehyde and Acetaldehyde. *Journal of Physical Chemistry*, 97:4293 – 4312, 1993.

[53] Willard M. St. John III, Ron C. Estler, and John P. Doering. Low-energy electron impact study of acetone*. *Journal of Chemical Physics*, 61(3):763 – 767, 1974.

[54] Ruth McDiarmid and A. Sablijć. Experimental assignments of the $3p$ Rydberg states of acetone. *Journal of Chemical Physics*, 89(10):6086 – 6095, 1988.

[55] James G. Foresman, Martin Head-Gordon, and John A. Pople. Toward a Systematic Molecular Orbital Theory for Excited States. *Journal of Physical Chemistry*, 96:135 – 149, 1993.

[56] T. H. Dunning. Gaussian basis sets for use in correlated molecular calculations. I. The atoms boron through neon and hydrogen. *Journal of Chemical Physics*, 90(2):1007–1023, 1989.

[57] David E. Woon and Thom H. Dunning Jr. Gaussian basis sets for use in correlated molecular calculations. III. The atoms aluminum through argon. *Journal of Chemical Physics*, 98(2):1358–1371, 1993.

[58] C. Hartwigsen, S. Goedecker, and J. Hutter. Relativistic separable dual-space Gaussian pseudopotentials from H to Rn. *Physical Review B*, 58:3641 – 3662, 1998.

[59] Gerald Lippert, Jürg Hutter, and Michele Parrinello. The Gaussian and augmented-plane-wave density functional method for ab initio molecular dynamics. *Theoretical Chemistry Accounts*, 103:124 – 140, 1999.

[60] P. E. Blöchl. Projector augmented-wave method. *Physical Review B*, 50(24):17953 – 17979, 1994.

[61] Matthias Krack and Michele Parrinello. All-electron *ab-initio* molecular dynamics. *Physical Chemistry Chemical Physics*, 2:2105 – 2112, 2000.

[62] Marcella Iannuzzi, Thomas Chassaing, Thomas Wallman, and Jürg Hutter. Ground and Excited State Density Functional Calculations with the Gaussian and Augmented-Plane-Wave Method. *Chimia*, (to be published), 2005.

[63] M. Petersilka, U. J. Grossmann, and E. K. U. Gross. Excitation Energies from Time-Dependent Density-Functional Theory. *Physical Review A*, 76(8):1212 – 1215, 1996.

[64] Rüdiger Bauernschmitt and Reinhart Ahlrichs. Treatment of electronic excitations within the adiabatic approximation of time dependent density functional theory. *Chem. Phys. Lett.*, 256:454, 1996.

[65] Christine Jamorski, Mark E. Casida, and Dennis R. Salahub. Dynamic polarizabilities and excitation spectra from a molecular implementation of time-dependent density-functional response theory: N_2 as a case study. *Journal of Chemical Physics*, 104(13):5134, 1996.

[66] Mark E. Casida, Christine Jamorski, Kim C. Casida, and Dennis R. Salahub. Molecular excitation energies to high-lying bound states from time-dependent density-functional response theory: Characterization and correction of the time-dependent local density approximation ionization threshold. *Journal of Chemical Physics*, 108(11):4439 – 4449, 1998.

[67] David J. Tozer and Nicholas C. Handy. Improving virtual Kohn-Sham orbitals and eigenvalues: Application to excitation energies and static polarizabilities. *Journal of Chemical Physics*, 109(23):10180 – 10189, 1998.

[68] So Hirata and Martin Head-Gordon. Time-dependent density functional theory for radicals An improved description of excited states with substantial double excitation character. *Chem. Phys. Lett.*, 302:375 – 382, 1999.

[69] Filipp Furche and Reinhart Ahlrichs. Adiabatic time-dependent density functional methods for excited state properties. *Journal of Chemical Physics*, 117(16):7433 – 7447, 2002.

[70] R. Eric Stratmann, Gustavo E. Scuseria, and Michael J. Frisch. An efficient implementation of time-dependent density-functional theory for the calculation of excitation energies of large molecules. *Journal of Chemical Physics*, 109(19):8218 – 8224, 1998.

[71] R. van Leeuwen and E. J. Baerends. Exchange-correlation potential with correct asymptotic behaviour. *Physical Review A*, 49(4):2421, 1994.

[72] John P. Perdew, Robert G. Parr, Mel Levy, and Jose L. Balduz. Density-Functional Theory for Fractional Particle Number: Derivative Discontinuities of the Energy. *Physical Review Letters*, 49(23):1691, 1982.

[73] Mel Levy, John P. Perdew, and Viraht Sahni. Exact differential equation for the density and ionization energy of a many-particle system. *Physical Review A*, 30(5):2745 – 2748, 1984.

[74] C.-O. Almbladh and U. von Barth. Exact results for the charge and spin densities, exchange-correlation potentials, and density-functional eigenvalues . *Physical Review B*, 31(6):3231, 1985.

[75] Axel D. Becke. Density-functional thermochemistry. III. The role of exact exchange. *Journal of Chemical Physics*, 98(7):5648 – 5652, 1993.

[76] Axel D. Becke. Density-functional thermochemistry. IV. A new dynamical correlation functional and implications for exact-exchange mixing. *Journal of Chemical Physics*, 104(3):1040 – 1046, 1996.

[77] Leonardo Bernasconi, Michiel Sprik, and Jürg Hutter. Time dependent density functional theory study of charge-transfer and intramolecular electronic excitations in acetone-water systems. *Journal of Chemical Physics*, 119(23):12417 – 12431, 2003.

[78] Hisayoshi Iikura, Takao Tsuneda, Takeshi Yanai, and Kimihiko Hiroa. A long-range correction scheme for generalized-gradient-approximation exchange functionals. *Journal of Chemical Physics*, 115(8):3540, 2001.

[79] R. T. Sharp and G. K. Horton. A Variational Approach to the Unipotential Many-Electron Problem. *Physical Review*, 90(2):317, 1953.

[80] James D. Talman and William F. Shadwick. Optimized effective atomic central potential. *Physical Review A*, 14(1):36 – 40, 1976.

[81] D. M. Bylander and L. Kleinman. The optimized effective potential for atoms and semiconductors. *International Journal of Modern Physics*, 10:399 – 425, 1996.

[82] Andreas Görling and Mel Levy. Exact Kohn-Sham scheme based on perturbation theory. *Physical Review A*, 50(1):196 – 204, 1994.

[83] A. Görling and M. Levy. DFT Ionization Formulas and a DFT Perturbation-Theory for Exchange and Correlation, Through Adiabatic Connection. *International Journal of Quantum Chemistry*, Suppl. 29:93 – 108, 1995.

[84] J. B. Krieger, Yan Li, and G. J. Iafrate. Construction and application of an accurate local spin-polarized Kohn-Sham potential with integer discontinuity: Exchange-only theory. *Physical Review A*, 45:101 – 126, 1992.

[85] Andrew M. Teale and David J. Tozer. Ground- and excited-state diatomic bond lengths, vibrational levels, and potential-energy curves from conventional and localized Hartree-Fock-based density-functional theory. *Journal of Chemical Physics*, 122:34101, 2005.

[86] Mark E. Casida, Kim C. Casida, and Dennis R. Salahub. Excited-State Potential Energy Curves form Time-Dependent Density-Functional Theory: A Cross Section of Formaldehydes $^1A_1$ Manifold. *International Journal of Quantum Chemistry*, 70:933 – 941, 1998.

[87] Mark E. Casida and Dennis R. Salahub. Asymptotic correction approach to improving approximate exchange-correlation potentials: Time-dependent density-functional theory calculations of molecular excitation spectra. *Journal of Chemical Physics*, 113(20):8918 – 8935, 2000.

[88] Oleg Gritsenko, Robert van Leeuwen, Erik van Lenthe, and Evert Jan Baerends. Self-consistent approximation to the Kohn-Sham exchange potential. *Physical Review A*, 51(3):1944, 1995.

[89] Oleg V. Gritsenko, Robert van Leeuwen, and Evert Jan Baerends. Direct approximation of the long- and short-range components of the exchange-correlation Kohn-Sham potential. *International Journal of Quantum Chemistry*, 61:231 – 243, 1997.

[90] O. V. Gritsenko, P. R. T. Schipper, and E. J. Baerends. Approximation of the exchange-correlation Kohn-Sham potential with a statistical average of different orbital model potentials. *Chem. Phys. Lett.*, 302:199 – 207, 1999.

[91] O. V. Gritsenko, P. R. T. Schipper, and E. J. Baerends. Ensuring Proper Short-Range and Asymptotic Behavior of the Exchange-Corelation Kohn-Sham Potential by Modeling with a Statistical Average of Different Orbital Model Potentials. *International Journal of Quantum Chemistry*, 76:407 – 419, 2000.

[92] Myrta Grüning, Oleg V. Gritsenko, Stan J. A. Gisbergen, and Evert Jan Baerends. On the required shape corrections to the local density and generalized gradient approximations to the Kohn-Sham potentials for molecular response calculations of (hyper)polarizabilities and excitation energies. *Journal of Chemical Physics*, 116(22):9591, 2002.

[93] S. J. A. van Gisbergen, V. P. Osinga, O. V. Gristenko, R. van Leeuwen, J. G. Snijders, and E. J. Baerends. Improved density functional theory results for frequency-dependent polarizabilities, by the use of an exchange-correlation potential with correct asymptotic behavior. *Journal of Chemical Physics*, 105(8):3142 – 3151, 1996.

[94] Leonardo Bernasconi, Michiel Sprik, and Jürg Hutter. Hartree-Fock exchange in time dependent density functional theory: application to charge transfer excitations in solvated molecular systems. *Chem. Phys. Lett.*, 394:141 – 146, 2004.

[95] Daniel Egli and Salomon R. Billeter. Analytic second variational derivative of the exchange-correlation functional. *Physical Review B*, 69:115106, 2004.

[96] Alan D. McNaught and Andrew Wilkinson. IUPAC Compendium of Chemical Terminology. online, http://www.iupac.org/publications/compendium/index.html, 2005.

Acknowledgments

I would like to thank Prof. Jürg Hutter and the Hutter group, present and former, for the nice time at the University of Zürich. In particular I want to mention Marcella Iannuzzi, who was a great help for the GAPW part, and Thomas Kastl, for the good company. I would also like to thank Stefan Jung for the friendship and the coffee.

I thank the CP2K team, especially Fawzi Mohamed, for the help with programming.

I am grateful to Johannes Neugebauer for providing me with ADF values of water and acetone.

Basis sets were obtained from the Extensible Computational Chemistry Environment Basis Set Database, Version 02/25/04, as developed and distributed by the Molecular Science Computing Facility, Environmental and Molecular Sciences Laboratory which is part of the Pacific Northwest Laboratory, P.O. Box 999, Richland, Washington 99352, USA, and funded by the U.S. Department of Energy. The Pacific Northwest Laboratory is a multi-program laboratory operated by Battelle Memorial Institute for the U.S. Department of Energy under contract DE-AC06-76RLO 1830. Contact Karen Schuchardt for further information.

Financial support from the Swiss National Science Foundation (Project 2000200-100417) is acknowledged.